Terrafirma: London H-3 Modelled Product. Comparison of PS data with the results of a groundwater abstraction related subsidence model.

Shallow Geohazards and Risks Programme

Commissioned Report OR/09/032

Terrafirma: London H-3 Modelled Product. Comparison of PS data with the results of a groundwater abstraction related subsidence model.

L B Bateson, A K A P Barkwith, A G Hughes and D T Aldiss.

Editor

A H Cooper

Keyworth, Nottingham   British Geological Survey   2009

BRITISH GEOLOGICAL SURVEY

The full range of our publications is available from BGS shops at Nottingham, Edinburgh, London and Cardiff (Welsh publications only) see contact details below or shop online at www.geologyshop.com

The London Information Office also maintains a reference collection of BGS publications, including maps, for consultation.

We publish an annual catalogue of our maps and other publications; this catalogue is available online or from any of the BGS shops.

The British Geological Survey carries out the geological survey of Great Britain and Northern Ireland (the latter as an agency service for the government of Northern Ireland), and of the surrounding continental shelf, as well as basic research projects. It also undertakes programmes of technical aid in geology in developing countries.

The British Geological Survey is a component body of the Natural Environment Research Council.

Contents

FIGURES

TABLES

1 Background to the study

A multi-disciplinary collaborative project funded by DEFRA and the Environment Agency investigated absolute changes in land level and in sea level around the United Kingdom during 1997-2005 (Bingley et al. 2007). The project comprised a national component, and a regional component in the London and Thames estuary area. It is the geological interpretation of the regional component that has been taken as a Terrafirma 'H2' product thereby forming the basis of the H3 work carried out and reported in this document.

The national component involved the serial measurement of land levels by absolute gravity (AG) and global positioning system (GPS) methods and of relative sea level change by analysis of tide gauge records. The estimates of change in land level from these two independent methods were combined as 'AG-aligned' GPS estimates of vertical tide gauge station velocity.

The national component of the project served to determine the average 'background' rate of sea-level change in British coastal waters, decoupled from changes in land level. It showed that this average change in sea level around Britain over a period of the past few decades, and possibly the past century, is a rise in the order of 1 mm/year. This is the component of sea level change that can be attributed to the consequences of global climate change.

The regional component of the project determined the absolute rate of land level change in the Thames estuary area. Serial measurements from local tide gauges and GPS data showed that the relative rate of sea level change in the Thames estuary for the past few decades to the past century has seen a 1.8 to 3.2 mm/yr rise in sea level with respect to the land along the Thames estuary and River Thames.

Furthermore, the regional component of the study included the determination of average ground velocity using PSI (persistent scatterer interferometry) techniques. In its conventional form, PSI provides a line-of-sight measurement (LOS) of ground motion displacements and average velocities relative to a ground reference point (assumed to have zero velocity), and to a single master satellite data scene, centred within the time period of data collection and which also minimises the perpendicular base-lines between the scenes. For this project, the PSI LOS velocities were re-projected to the vertical. The velocities were also corrected to the AG-aligned GPS determinations, so providing a measure of absolute ground motion, relative to the geoid, for the period of the project.

For the study of the Thames estuary area, the area of the PSI data was approximately 95 x 55 km in extent, aligned with the satellite track, centred on central London. This area encompassed a network of three CGPS and 12 EGPS stations, established in 1997. A total of 82 descending ERS and ENVISAT SAR scenes (Track 51, Frame 2565) spanning nearly nine years (March 1997 to December 2005) were processed by Nigel Press Associates, generating a dataset of about 950 000 PS points (Bingley, et al., 2007; 2008).

The estimate of the rate of change in land level for each PS point was plotted to produce a detailed high resolution map of current rates of land level change in the London area. This map was subjected to geological interpretation by the British

Geological Survey, partly to validate the PSI data and partly to identify local and regional patterns of ground movement, and also the processes that control the rate of land level change.

The geological interpretation demonstrated that the PSI data is non-random, and so is a valuable tool for assessing patterns of modern ground movement, especially when aligned with measures of absolute ground movement. It also demonstrated a variety of controls on the rates of land level change, ranging from less than a decade to more than 100 000 years' duration.

During the period 1997 to 2005, the region around the Thames estuary subsided mostly between 0.9 and 1.5 mm/year, but in some areas as fast as 2.1 mm/year. These rates of subsidence are close to values determined by previous studies of Quaternary sequences, but the AG/GPS-aligned PSI data demonstrate a level of local structural control that cannot be resolved by other methods. Furthermore, the AG/GPS-aligned PSI data showed that an area of west London is rising at about 0.3 mm/year, which had been undetected by other techniques.

The short-term controls on land level change are anthropogenic and give rise to some of the fastest rates of change, but their effects are confined to fairly small areas. The largest areas of most rapid subsidence (as fast as 2.1 mm/year) coincide with the thicker (more than about 5 m) deposits of Holocene alluvium on the River Thames flood plains (Figure 1). Some areas of old artificial ground (as at the Dagenham motor works) are subsiding at the regional rate, consistent with accelerated compaction of reclaimed flood plains ceasing after about 50 to 100 years. Narrow zones of most rapid subsidence mark sites of recent tunnelling works, as for the Jubilee Line Extension under Westminster.
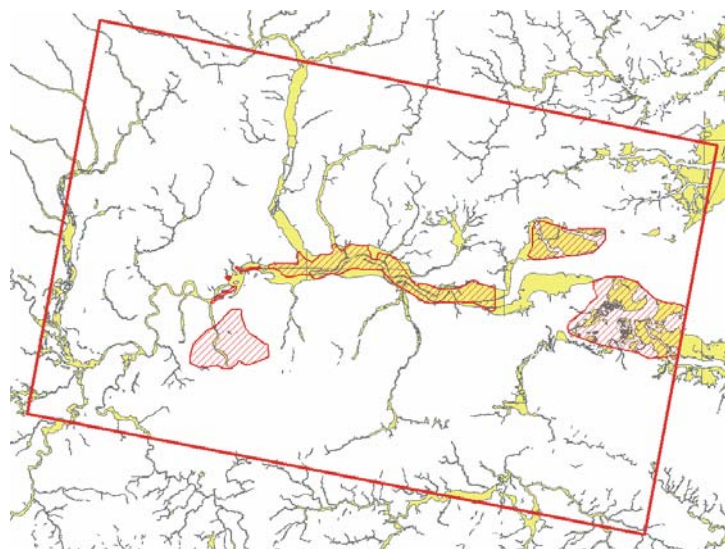
Figure 1. Areas of most rapid subsidence (red hatching) compared with Holocene alluvium on the flood plains and salt marshes (shown in yellow). The area of InSAR processing is shown by the red bow, which is 90km by 60km.

When the effects of near-surface, short term localised subsidence are disregarded, a broad pattern of regional changes emerges. This pattern is related to geological

structures within the pre-Mesozoic basement (at depths of c. 200 m to 2000 m). It is centred on parts of west and north London which subsided by less than 0.7 mm/year, and which in one area rose by about 0.3 mm/year. This part of the region lies on the Midlands Microcraton (a region of very long-term relative crustal stability). Rates of subsidence generally increase to the east, off the edge of the microcraton. A major lineament in the ground velocity data lies parallel to basement structures, indicating long-term deep-seated control on local subsidence patterns (Figure 2).
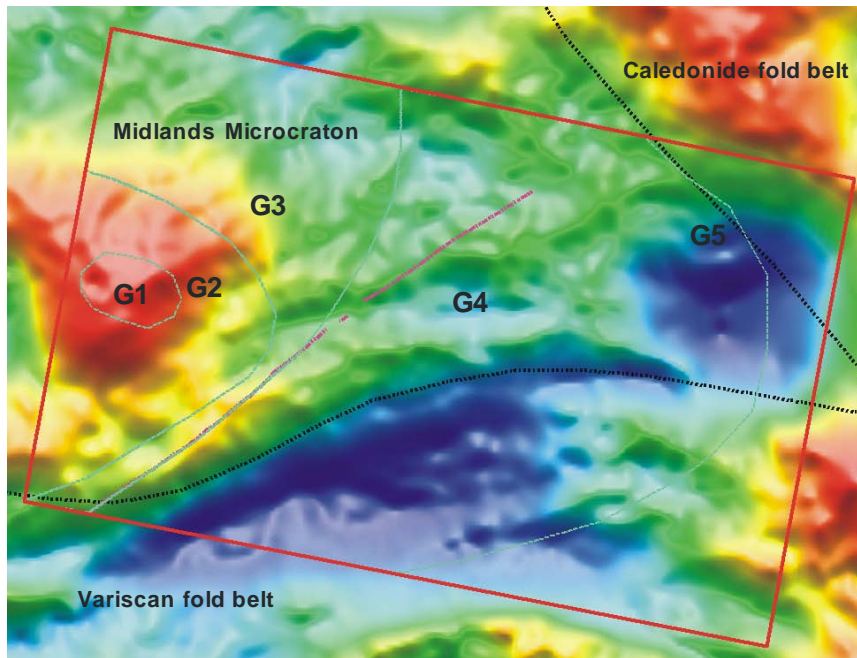
Figure 2. Residual Bouguer gravity anomaly map with generalised ground velocity domains (G1 to G5). The area of InSAR processing is shown by the red bow, which is 90km by 60km.

One of the most striking correlations between local variation in land level change and local geological processes was found in the Merton area of south-east London, which subsided some 0.5 mm/year faster than the surrounding area between 1997 and 2005 (Figure 3). Here, groundwater levels have been lowered by at least 30 m during the same period, as a consequence of abstraction at the Merton Abbey public water supply well, one of a number of sites in this part of the London area where water is taken from the Chalk at depths in excess of 70 m.
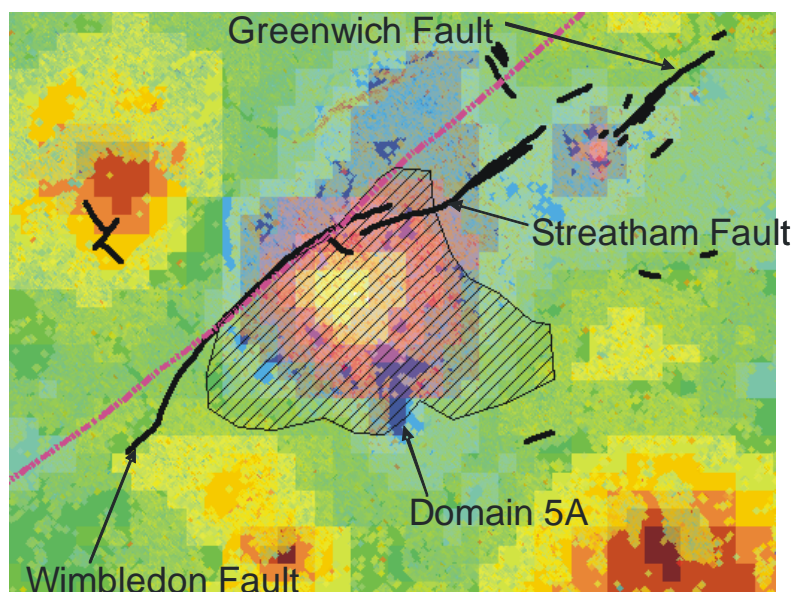
Figure 3. Ground subsidence in the Merton Abbey area (black hatching) and changes in water table level. Area of black hatching is 11km across.

The north-west edge of the area of anomalous subsidence around Merton Abbey is coincident with the Wimbledon Fault, and it appears that fractures parallel to the Wimbledon Fault are exerting some control on groundwater movement.

It is the Merton Abbey area that was chosen as the subject of the Terrafirma H3 modelled product; a quantitative analysis of the relationship between a local anomaly in rates of land level change, as shown by the PSI data, and the inferred causal mechanism.

2 The hydrogeology of the London Basin

To provide context for the relationship between groundwater head decline and ground surface movement, it is necessary to provide a background to the hydrogeology of the London Basin. A brief summary of the Thames Basin geology relevant to the study area is provided, followed by a discussion of the hydrogeology and the control of rising groundwater.

2.1   GEOLOGY OF THE LONDON BASIN

The geology of the London Basin that is relevant to the discussion of compaction is summarised in Table 1. This table provides a description of the Cretaceous and Palaeogene age deposits present in the London Basin, and is based on the London Memoir (Ellison et al., 2004). The main geological units of relevance are; the Chalk Group, generally comprising a white micro-porous limestone, the Thanet Sand Formation (so-called "basal sands"), the Lambeth Group and the Thames Group including the London Clay formation. The Thames Basin has a number of faults and

folds which together produce the basin structure.   The main synclinal axis is orientated in a west-south-west to east-north-east direction.   The deepest part of the basin is found to the west of London, under Walton-on-Thames. Figure 4 provides a simplified cross-section of the London Basin which summarises all the features outlined above.
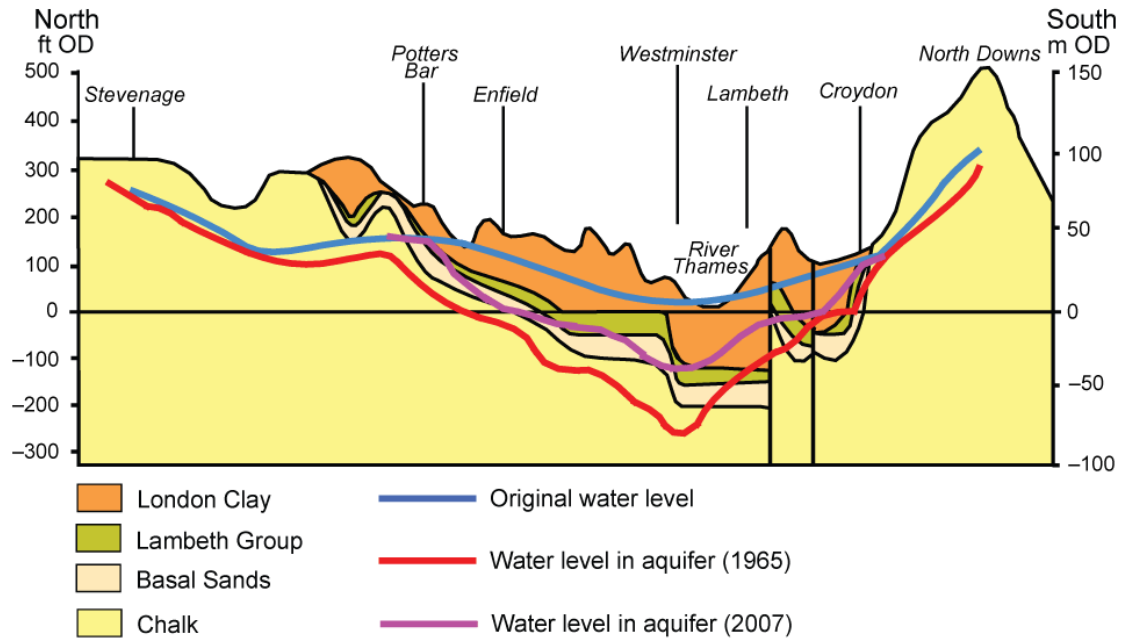
Figure 4. Schematic cross section of the London Basin. Copyright BGS/NERC. (from the Groundwater Forum website – accessed 30/3/2009).

Table 1.   Summary of the geology of the London Basin

Period	Group	Formation	Thickness (m)
PALAEOGENE		BAGSHOT FORMATION: sand, fine-grained with thin clay beds	10–25
	THAMES	LONDON CLAY FORMATION: clay, silty; fine sand clay at base.	90–130
		HARWICH FORMATION: sand, clayey fine-grained sand and pebble beds	0–10
	LAMBETH	READING, WOOLWICH and UPNOR formations: clay mottled with fine-grained sand, laminated clay, flint pebble beds and shelly clay	10–20
		THANET SAND FORMATION: sand, fine-grained	0–30
CRETACEOUS	CHALK	Undivided mainly SEAFORD CHALK FORMATION: chalk soft, white with flint beds	Up to 70
		LEWES CHALK FORMATION: chalk, white with hard, nodular beds	25–35
		NEW PIT CHALK FORMATION: chalk white to grey with few flints	30–40
		HOLYWELL CHALK FORMATION: chalk white to grey, shelly, hard and nodular	13–18
		Undivided ZIG ZAG CHALK FORMATION and WEST MELBURY MARLY CHALK FORMATION (formerly Lower Chalk): chalk, pale grey with thin marls; glauconitic at the base	65–70
		UPPER GREENSAND FORMATION: sand, fine-grained, glauconitic	Up to 17
		GAULT FORMATION: clay, silty	50–70
	LOWER GREENSAND	FOLKESTONE FORMATION: sandstone, fine- to medium-grained	60

9

2.2   HYDROGEOLOGY OF THE LONDON BASIN

Chalk is the principal aquifer of the London Basin. This sequence is confined by the London Clay over much of the area. It is in hydraulic continuity with the overlying sands of the Thanet Sand and Upnor formations (see Table 1), which together are commonly referred to as the 'Basal Sands'. This aquifer is fed by the outcrops of the Chalk aquifer to the north of London (Chilterns Hills) and to the south of London (North Downs) (Figure 4). Groundwater flow occurs towards the centre of the London Basin.

Groundwater has been exploited from the Chalk in the London Basin since the mid-1850s. Large diameter wells were dug through the London Clay to the underlying basal sands and Chalk to allow abstraction from the Basal Sands and the Chalk aquifers. However, after the Second World War, groundwater abstraction in the centre of London started to decline. There were a number of reasons for this, including reduced yield from the wells, a switch to surface water sources, the move of industry to the outskirts of London, and the effects of bombing in the war itself.

The reduction in groundwater abstraction has led to rising groundwater levels within the London Basin. This has caused concern amongst the London authorities that tunnels, deep basements and foundations for tall buildings will be flooded. The rise in groundwater levels in London can be illustrated by the groundwater hydrograph at Trafalgar Square (Figure 5). This hydrograph, which is considered representative of London Basin groundwater levels, shows that the level was in decline until the 1950s and started to rise again after the mid 1970s. This rise in groundwater stabilised after 2000 due to a combination of climatic conditions and a strategy to control the rise by increased groundwater abstraction.

2.3   CONTROL OF RISING GROUNDWATER

To counter the rise in groundwater a strategy was developed to reduce the inflow of groundwater into the centre of the London Basin. This strategy, produced by the General Aquifer Research, Development and Investigation Team (GARDIT), involved increasing groundwater abstraction in five phases. These phases included; re-commissioning disused abstractions, refurbishing existing abstractions, enhancing the yield from private boreholes, and drilling new sites in the centre of London.

In general, demand for groundwater continues to rise in London as the per capita water usage increases. This means that new sites are being developed and existing ones are increased. This fact combined with the implementation of the GARDIT strategy means that groundwater abstraction in various parts of London is increasing. According to the Environment Agency (2007), licensed groundwater abstraction has increased from 80,000 Ml/a in 1990 to nearly 130,000 Ml/a in 2006. It is the increase in abstraction around the Abbey Fields pumping station that has led to a localised decline in groundwater levels and subsequent compaction of the ground surface.
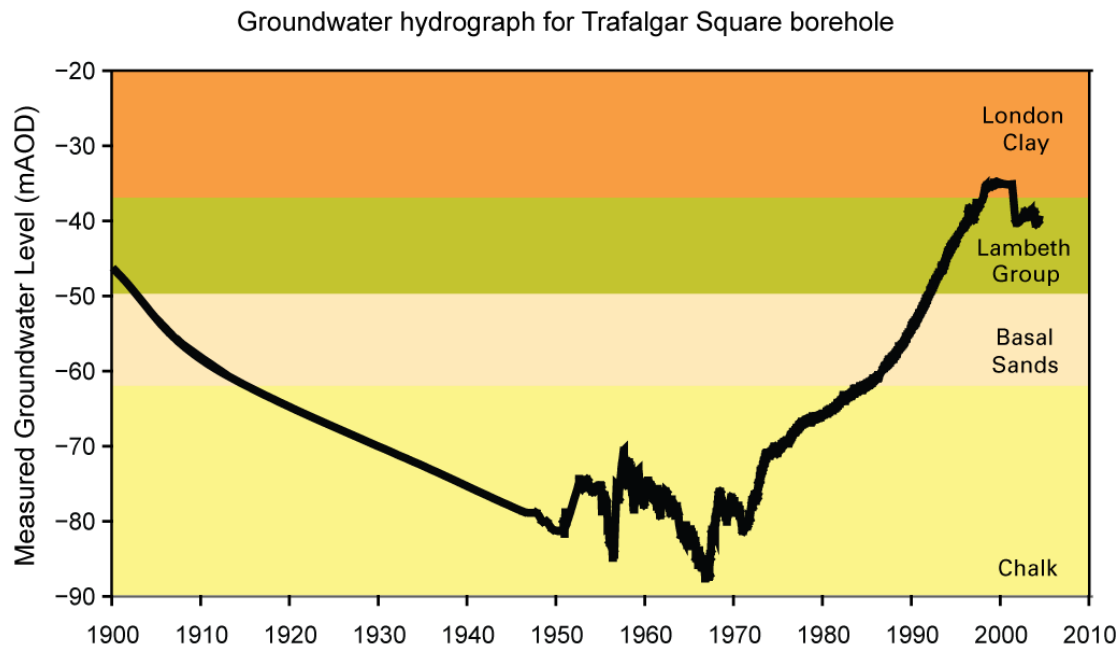
Figure 5. Groundwater hydrograph for Trafalgar Square borehole, Copyright BGS/NERC (from the Groundwater Forum website – accessed 30/3/2009).

3 A simplified model to relate land subsidence and groundwater level.

3.1   INTRODUCTION

It has long been recognised that a reduction in groundwater level can result in the compaction of strata and subsidence of the overlaying terrain. The amount of compaction, due to a change in hydrostatic pressure, is dependent on the physical properties of; the rock matrix, the geological setting of the strata, and its hydrological history.

This section describes a new simple model that calculates the amount of strata compaction which may result from reduction in piezometric head. The complex nature and required level of data needed to run current numerical subsidence models makes them costly in terms of time and required resources. A simplified model was created to study the relationship of groundwater levels to observed subsidence, which was centred on the Croydon area of the Thames Basin. Over recent years, this area recorded an average drop in groundwater of up to 10 m/year in response to the GARDIT strategy (see section 2.3).

3.2   PHYSICAL CONCEPTS

This model is based on the effective stress principle proposed by Terzaghi (1925). As a formation is laid down and subsequently overlain by more material, the geostatic pressure (p) increases. The geostatic pressure is resisted by a combination of the fluid pressure of the pore water (p_w) and the intergranular (effective) stress (p_s) within the rock matrix (Shearer, 1998). A reduction in piezometric head, reduces the pore fluid pressure and increases the effective stress on the matrix. The relationship can be equated as;

Equation 1 $$p_s = p - p_w$$

The initial ratio of pore fluid pressure to effective stress can be approximated from work by Poland (1984). For an unconfined aquifer, the geostatic pressure is divided as; p_s (60%) and p_w (40%). For a confined aquifer the geostatic pressure is divided as; p_s (75%) and p_w (25%), see Figure 6. Poland (1984) calculated that a 1 m fall in piezometric head results in a 10 kPa reduction in the pore fluid pressure.
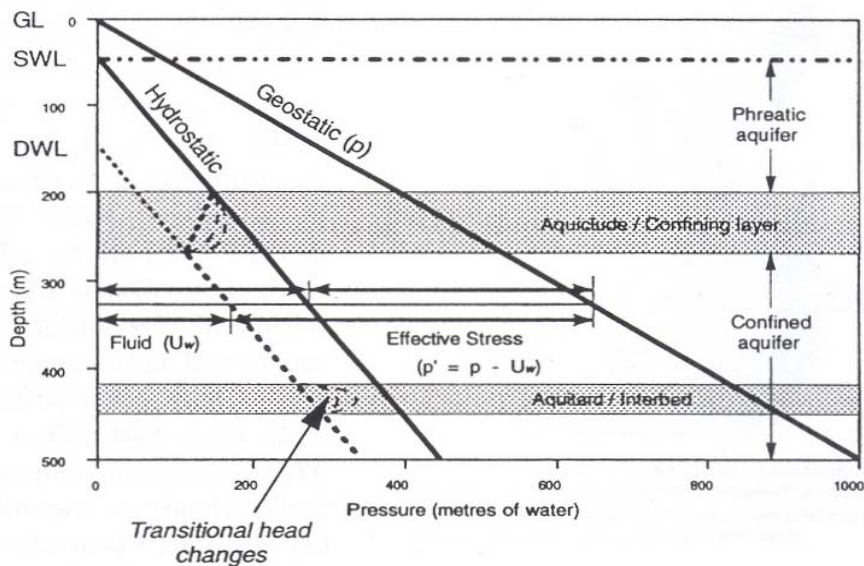
Figure 6. Initial effective stress calculation as a percentage of geostatic pressure for both unconfined and confined aquifer environments (Shearer, 1998; after Poland, 1984).

Equilibrium in Equation 1 must be maintained; hence compaction occurs until the matrix is dense enough to once again support the overlaying material. For coarse grained strata (sand, gravel, etc), the rigid *skeleton* of the matrix is often strong enough to maintain equilibrium with low levels of compaction. Fine grained strata (clay) however, respond to increases in effective stress with relatively high levels of *potential* compaction due to their plastic nature. Meinzer (1928) recognised the increased compaction potential of low permeability beds, specifically those with high clay content.

The compaction response of strata to change in piezometric head is highly dependent on the previous history of the pressure changes. Variations in effective stress within the limit of previous small-scale changes (i.e., seasonal) are recoverable (elastic), allowing the system to expand/contract by small amounts. When a change in head far exceeds the previous small-scale variations, a much greater compaction occurs. This compaction is non-recoverable (inelastic) and limits any further compaction to the affected strata.

The permeability related time delayed response of compaction to head change was calculated by Jacob (1940), who deducted: The low permeability of clay layers would result in slower drainage than in the coarser aquifer material and that longer term transitional head changes would introduce a time delay between the extraction (of groundwater) and the consequent compaction (Shearer, 1998). The aquitard time constant, τ (Riley, 1969), is used to calculate the time it takes a bed to reach equilibrium following an instantaneous change in pressure;

Equation 2
$$\tau = \frac{Ss(b)^2}{k_z},$$

where, k_z is the vertical conductivity, b is the thickness of the unit, and Ss is the specific storage, which is a function of; difference in bed thickness (Δb), and difference in head (Δh). For a consolidating bed, S_w can be considered as zero and hence ignored (Poland, 1984);

Equation 3 $$Ss = \frac{\Delta b}{b \Delta h} + S_w$$

3.3 MODEL EQUATIONS

The simple formula on which the model is based has been presented before (Terzaghi, 1925; and Poland, 1984), however it has largely been negated since the introduction of complex numerical models and increased levels of computational power. The total difference in bed thickness, after an instantaneous change in effective stress has been applied, is calculated as a function of, *coefficient of volume compressibility* (m_v) and initial thickness (b_0);

Equation 4 $$\Delta b = m_v \Delta p_s b_0$$

The coefficient of volume compressibility is a term often used in the field of soil mechanics, relating, the coefficient of compressibility (a_v) and the initial void ratio (e_0). It is defined as;

Equation 5 $$m_v = \frac{a_v}{1 + e_0},$$

where;

Equation 6 $$a_v = \frac{\Delta e}{\Delta p_s},$$

and;

Equation 7 $$e = e_0 - c_c \log\left(\frac{p_s}{p_{s0}}\right),$$

So that the *new* void ratio (e) is expressed as a function of; the initial void ratio, the *compressibility index* (c_c), the initial and new effective stresses. The initial void ratio is simply derived from initial porosity (n_0);

Equation 8 $$e_0 = \frac{n_0}{1 - n_0}$$

The compressibility index (dimensionless) represents the compressibility of the unit being studied. It can be calculated using Equation 6 if the new void ratio is known. If the model is intended for prediction use (i.e. the compaction has not yet taken place), the compressibility index can be

derived from laboratory based, deformation testing of samples. The acquisition of, and testing of samples is costly, therefore this may not be a viable option. Under these circumstances, compressibility index may be approximated using studies which link groundwater extraction to subsidence in other regions to calibrate the model. These studies may be either measurement based, or based on the results of current complex numerical simulations. The compressibility index takes the elastic properties of the units being studied into account. If the approximation through calibration method is used, then it is important that the groundwater history of each case is established, as only those with similar compaction history (either elastic or inelastic) should be used.

3.4   SIMULATION

The simple model was constructed using Microsoft Excel. Limitations imposed by the architecture of the software and the project, require a simplification of the geological setting. The model is designed to calculate the amount of compaction for an individual formation. The total amount of compaction will be a combined total of each formation compaction. Each of the formations were assumed to contain a homogeneous matrix and each assigned an average density and initial porosity based upon sediment type and depth of burial (see Zimmerman, 1991). The compression indices were derived from the calibration technique, by comparison to several subsidence measurement studies (Shi *et al.*, 2007; Kitching and Shearer, 1995; Bell *et al.*, 1986; and Poland, 1984). The initial thickness of each formation for a particular reference point was estimated using the London Basin 3D model constructed using GSI3D. The overburden depth for each formation was calculated as; the depth of the overlying material plus half the depth of the formation being studied (Figure 7). This is to account for the geostatic pressure of a formation upon itself. The model uses the known transfer of stress from fluid to matrix per unit change in groundwater level (10 kPa/m) to calculate the change in effective stress, the new void ratio (Equation 6), and the amount of compaction that occurs (Equation 3).
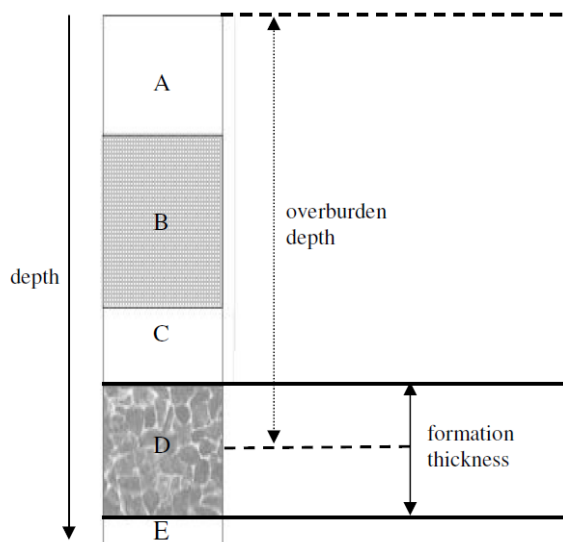
Figure 7. Schematic diagram of 5 formations (A-E). The overburden depth is; the thickness of the material overlaying the formation plus half of the formation thickness that the model is being run for. This is highlighted for formation D.

The use of macros allows the model to be run for any number of time steps, the size of which are defined by the rate of piezometric head reduction. For example, if the rate is input as 10 m/year, each time-step would advance the model by a single year. If the rate was input as 0.83 m/month (the same flow rate per year), each time-step would advance the model for one month. As the model time-step is advanced, it recalculates the new formation thickness, void ratio, and compaction. It is therefore beneficial to increase the number of time steps for a set period of time. A monthly rate was found to be the best compromise between time and resolution. As the formations are considered homogeneous, and the water removal is considered as a rate of piezometric head reduction (m/time), and not a quantity removed (m^3), the time-lag constant (Equation 2) is not considered in the model. It is however possible to apply the time-lag constant to the output after the model if an approximation of the time-lag is required The model outputs for each time-step; time (months), cumulative piezometric head reduction (m), formation thickness (cm), change in thickness (mm), and cumulative change in thickness (mm). It also has the option of running 12 time-steps (one year) simultaneously and only outputting the final step. It should be noted that the rate of piezometric head reduction may be altered between time-steps allowing the simulation to handle *real-world* rate changes (for example; variable pumping rates).

For the Terrafirma study, three test cases were conducted using differing temporal resolutions of groundwater level fluctuation:

1. **Case 1** required the model to be run using a 9 year averaged drop in head for various locations on the north-south east-west intersecting trend lines. For each location the 9 year average was divided into monthly rates, and the model run for the 9 year duration. Computation using constant piezometric levels is not a strain on user time or computation resources, and therefore it was possible to run the model for a large number (23) of sites.

2. **Case 2** used yearly averages of groundwater level for the model runs, which were again divided into monthly rates. The increased complexity and hence time in running the model allowed only a reduced number (6) of locations to be studied.

3. **Case 3** focused on a single location, close to the centre of the area of study. Here monthly rates of head fluctuation were used, based upon measured levels from a groundwater pumping station (Merton Abbey). This run was labour intensive and required a lot of user interaction to derive the compaction results.

3.5   SAMPLE MODEL RESULTS

The results from a single location are presented for each of the test cases. Although these are not all at the same location, they are within close proximity of one another. Table 2 shows the constants used to determine the compaction rates for each formation. The constants used are approximations derived from comparison studies within the literature (Dobrynin, 1962; Gupta and Larson, 1979; Poland, 1984; and Zimmerman, 1991). It should be noted that the London Clay is included for its overburden properties, hence not all of the constants are needed. The variable formation thicknesses and model groundwater rate changes for each case are given in Table 3.

Formation	Density (kg/m^3)	Compression Index	Porosity
London Clay (LC)	1750	----	----
Lambeth Group	1800	0.0025	0.35
Thanet Sands	2000	0.0015	0.3
Chalk Group	2800	0.001	0.55

Table 2. Constants used for the Terrafirma model runs.

Case # (location)	Case 1 (3,-2)	Case 2 (4, -2)	Case 3 (MA)
GW rate resolution	9 year avg	1 year avg	monthly
LC thickness	15.57	33.48	30.53
Lambeth thickness	11.98	10.18	12.60
Thanet thickness	10.20	9.42	12.91
Chalk thickness	201.09	210.43	196.70

Table 3. Formation thicknesses (m) for the locations and the groundwater temporal resolutions used for each case. Case 3 is located at Merton Abbey (MA).

3.5.1   Case 1

The compaction results from location (3,-2) are presented in Figure 8. During 9 years of measurement, the piezometric head has been reduced by 30.68 m, giving a monthly groundwater fall rate of 0.28 m. This rate was kept at a constant for the duration of the run. Most compaction (6.79 mm) is exhibited by the Lambeth Group, which contains a relatively high percentage of fine clay material. The total compaction of the Chalk formation (4.93 mm) is due to its large thickness. The least compaction (3.25 mm) is experienced in the Thanet Sands, which have a low compression index and formation thickness. The total compaction predicted at this location is 14.98 mm over the 9 year period with a constant groundwater reduction rate.
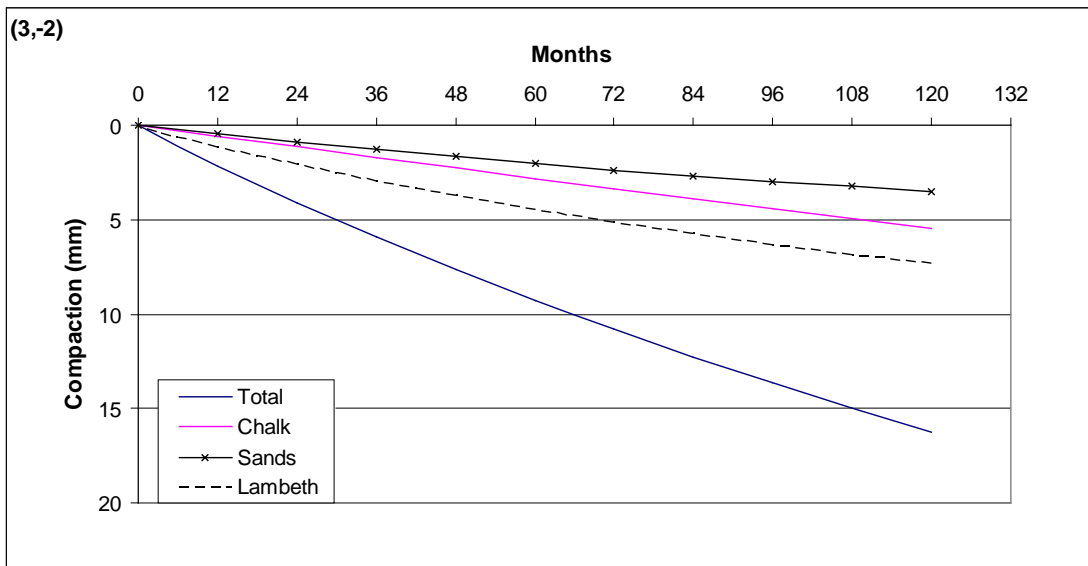
Figure 8. The modelled compaction for location (3,-2). The graph includes the results for each modelled formation and the total predicted compaction. The piezometric level is reduced by 30.68m over 9 years.

The total compaction at the other locations used in case 1, range from 7.02 mm to 26.06 mm, with the drop in piezometric level being the most influencing factor. The model predicts smaller compaction rates where there is a larger overburden, in areas with similar groundwater reduction rate. This fall in compaction rates has the most pronounced effect on the Lambeth Group. The

amount of overburden also affects the linearality of the results, with less overburden creating increased compaction rates which reach steady state over time.

3.5.2   Case 2

For case 2, the model was allowed to run for 24 months at a predetermined rate; to lessen the impacts of the initial increased compaction experienced in case 1. The groundwater level (Figure 9) was changed on a yearly basis during model execution, the results of which are presented (Figure 10) for location (4, -2). As the model does not include any time-lag element, it follows the same trend as the groundwater fluctuations. At this location the compaction of the Lambeth Group and Thanet Sands are relatively small, only totalling 3.70 mm. The total compaction, including the Chalk, predicted by the model is 6.69 mm over the 5 year running period (1997 - 2001).
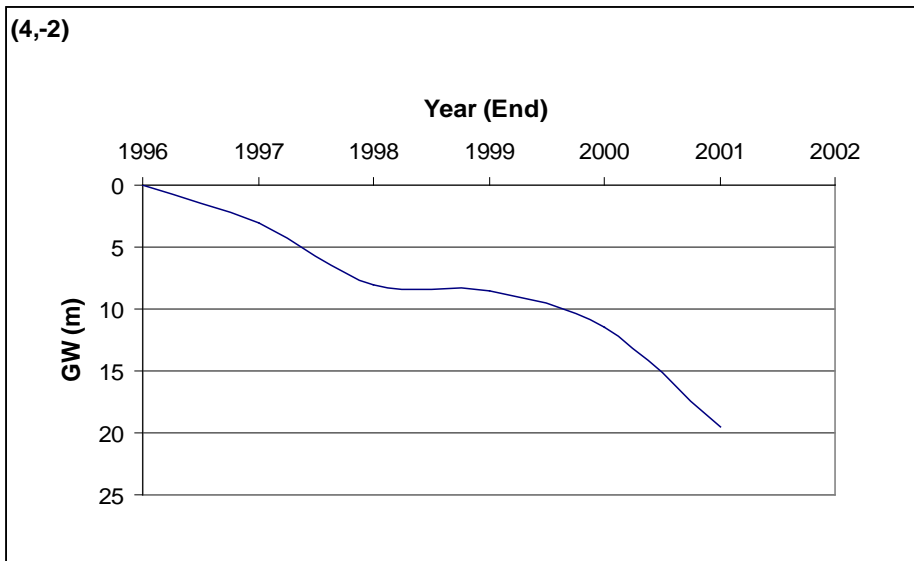
Figure 9. Yearly piezometric head levels over a 5 year period for location (4,-2).
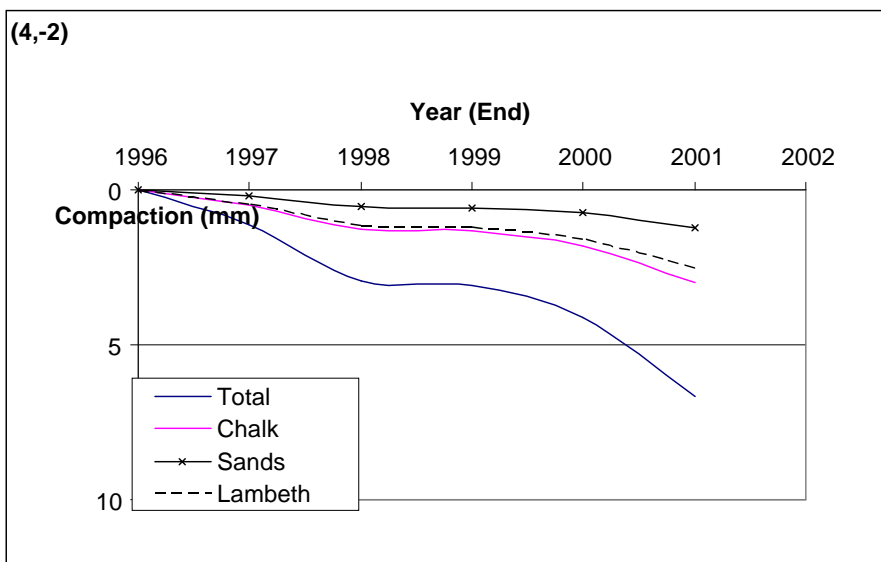
Figure 10. Predicted compaction (mm) over a 5 year period for location (4,-2). The groundwater level fluctuations were changed yearly.

18

3.5.3   Case 3

For the Merton Abbey case, the groundwater fluctuation is updated monthly over the 13 year period between 1993 and 2005. The piezometric head (Figure 11) exhibits large fluctuations (up to 55 m) over timescales of a month.
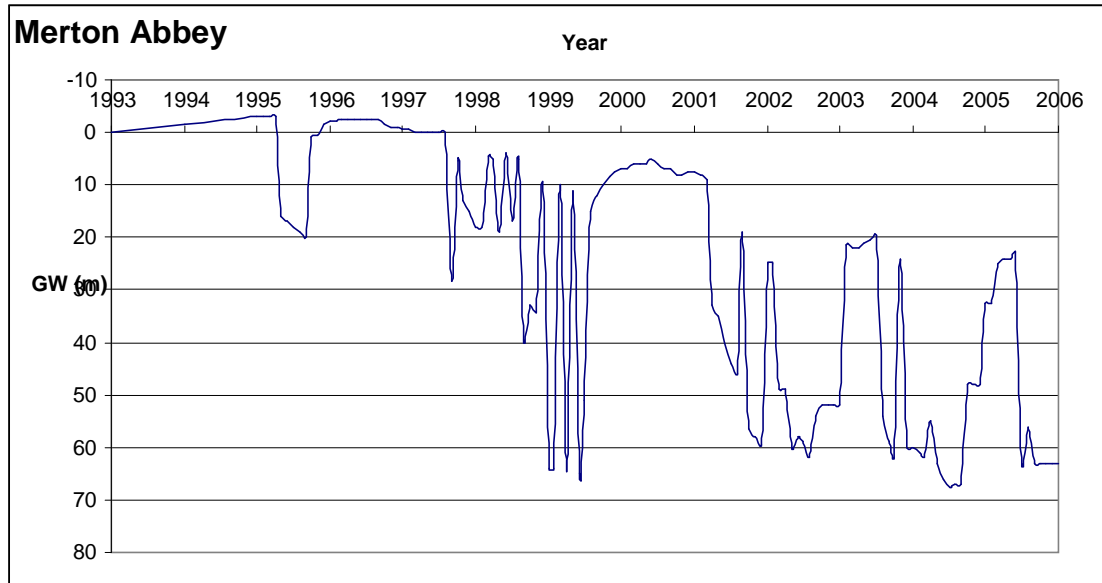
Figure 11. Monthly piezometric head levels over a 13 year period for the Merton Abbey pumping station.

The compaction predicted by the model over the 13 year pumping period for Merton Abbey is given in Figure 12. As no time-lag constant is used, the modelled variation in compaction rate varies considerably on a monthly scale, in-line with the groundwater levels that were input. The compaction rates from this case use 1993 as the datum. In December of 2005 a total compaction of 21.15 mm is predicted. The maximum compaction of 22.29 mm is predicted in June 2004. Between 1993 and 1997, a period of uplift is predicted by the model in response to an increase in piezometric level.
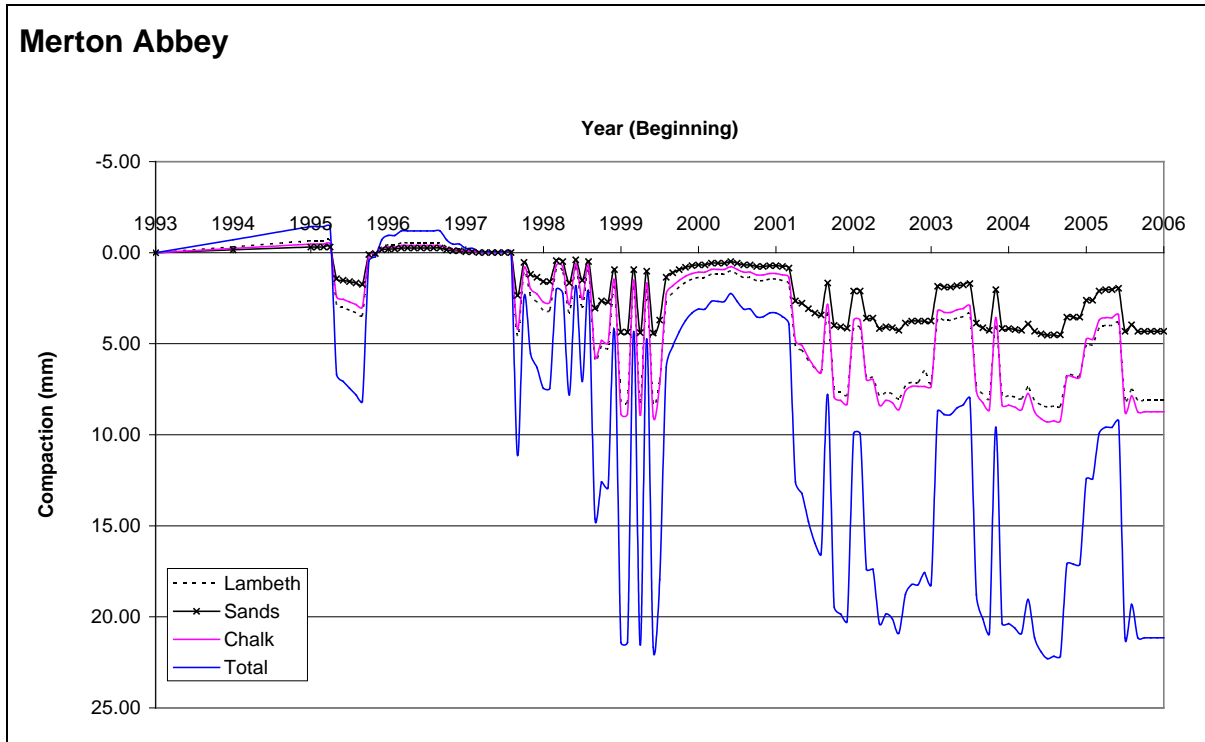
Figure 12. Monthly predicted compaction (mm) over a 13 year period for the Merton Abbey pumping station.

4 Comparison of the Modelled ground motions with PS terrain motions

4.1   INTRODUCTION

The comparison of the subsidence model results and PS subsidence has been conduced for the Merton area of south-west London. The study area, as outlined in Figure 13 corresponds to domain 5a from the London land-levels work, where an overall subsidence rate of -1.55 mm/yr is associated with groundwater abstraction (Bingley et al, 2007).
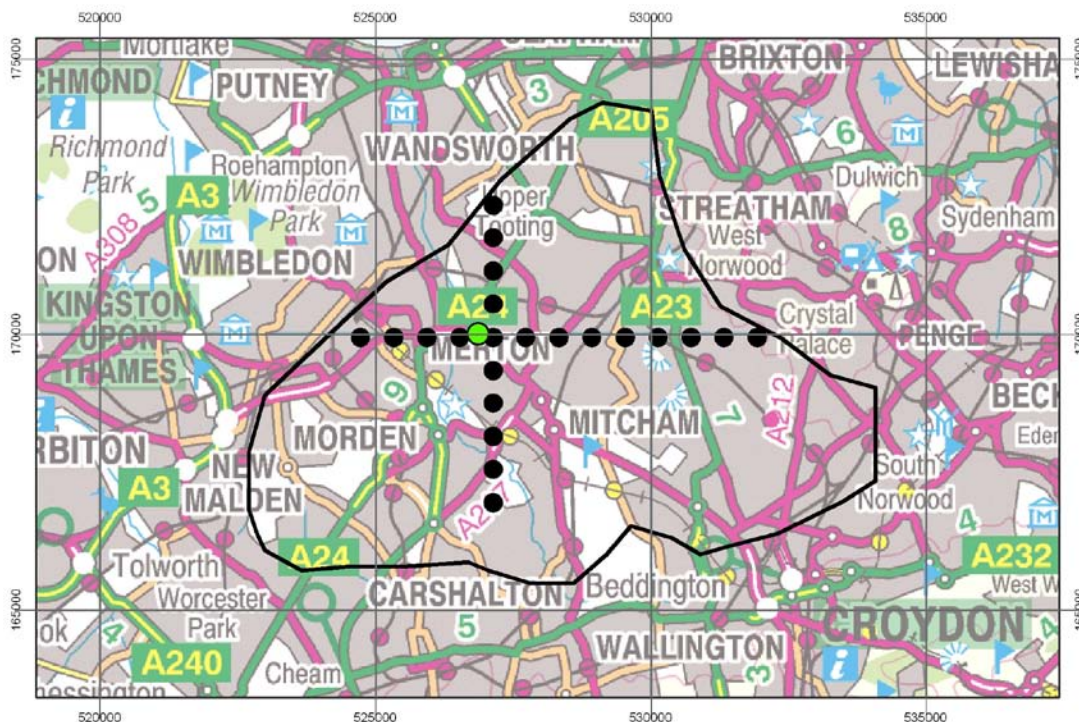
Figure 13. The study area in the Merton Area of London. Also shown are the comparison points in black and the location of Merton Abbey pumping station (green).

The comparison has been completed at the three temporal resolutions stated in section 3.4, namely case 1, 2 and 3.

4.2   DEFINITION OF COMPARISON POINTS

The ground water related subsidence model is designed to be run for a single location; the PS dataset is a point dataset. It was therefore decided to complete the comparison using several points. The definition of suitable comparison points was achieved by interpreting the average (1997 to 2006) groundwater level change dataset (Figure 14).
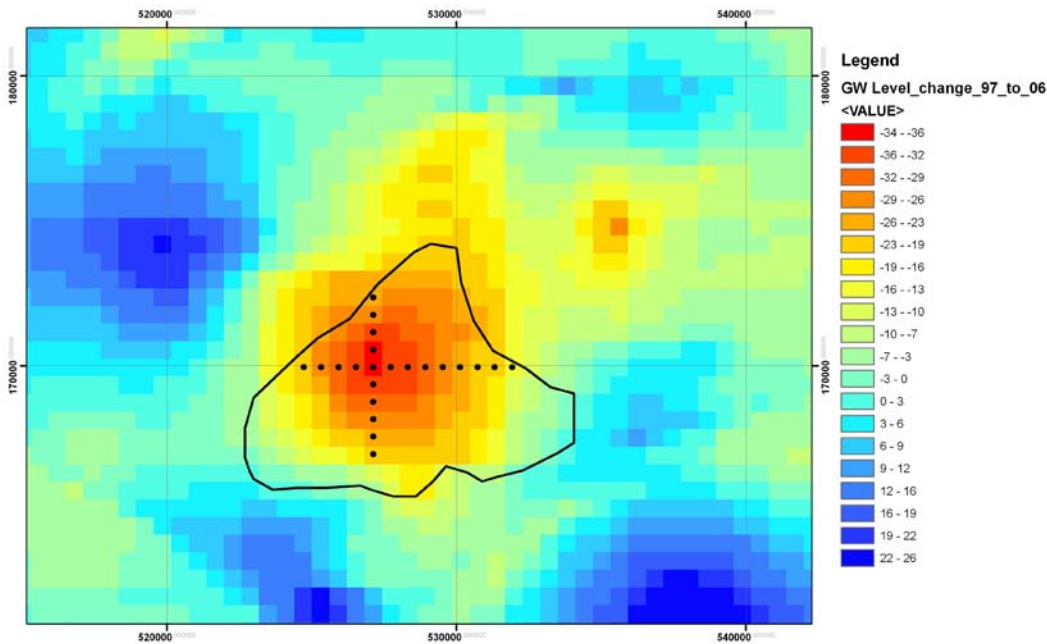
Figure 14. The comparison points used. Background is the average groundwater level change from 1997 to 2006, the black polygon is the groundwater domain identified in the London land-levels project and forms the study area for this comparison.

22 points centred on the area of maximum groundwater level change and extending to the areas of minimum groundwater level change were used. Comparison points are 600 m apart, corresponding to the cell size of the groundwater dataset, each point is therefore at the centre of a cell. A two-digit reference is given to each point this relates to its position in the cross. The central point would have been (0,0) however re-evaluation of the origin means that the horizontal axis is at the -2 level therefore the central point is (0,-2). The most easterly point is (8,-2), the most westerly point is (-4,-2), the most southerly is (0,-7) the point furthest to the north is (0,2).

The comparison for case 1, the study period average, is completed for each of the 22 comparison points. Due to the length of time required to run the model, comparisons for case 2 are completed on 6 of the points (Figure 15). The reasons for the selection of each of these points are given in Table 4.

Point ID	Reason for selection
0,0	Has a high groundwater level change for each date
0,2	Next to fault
0,-7	Largest difference in groundwater levels between years
4,-2	Represents edge of the subsidence area, relatively low subsidence
-4,-2	Represents edge of the subsidence area, relatively low subsidence
8,-2	Has a Low groundwater level change for each date

Table 4. Reasons for the selection of points for yearly comparison.

For case 3, the monthly comparison was completed just for the location of the Merton Abbey pumping station (Figure 15).
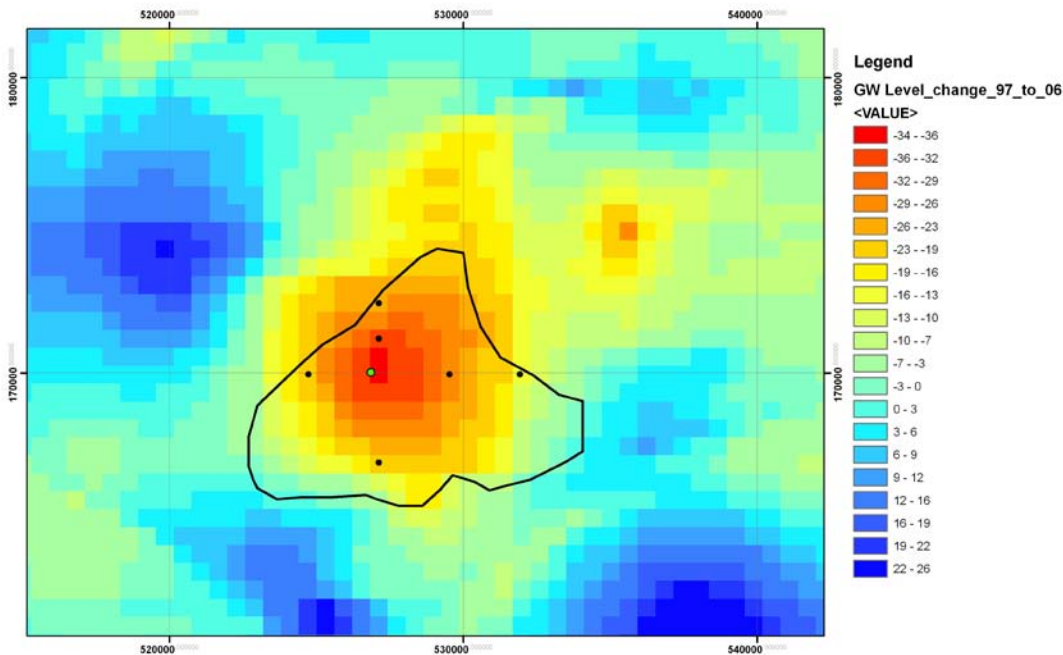
Figure 15. Location of the points used for the yearly comparison (black) and the location of Merton Abbey (green) used for the monthly comparison.

Merton Abbey pumping station is the name of the location of the borehole where the ground water affecting this region is withdrawn. It is also where the Environment Agency make there ground water level measurements for the region. Merton Abbey pumping station is 6 km north of Sutton and has a grid reference of TQ 2686, 7001. These are the measurements used as input to the subsidence model and therefore a direct comparison in this location was likely to give the most accurate model results.

4.3   INPUTS TO THE SUBSIDENCE MODEL

The subsidence model, as described in section 3, requires the following input for each location:

- Accurate thickness of underlying geological units

- The change in groundwater level

- Geological characteristics

4.3.1   Thickness of underlying geological units

Geological unit thicknesses were derived from the BGS London LithoFrame 50 geological model (Figure 16). This 1:50,000 scale model has been created from 1:10,000 scale field mapping and borehole data and as such is an accurate representation of the subsurface geology. The model is viewed and interrogated in the GSI3D subsurface viewer (Terrington et al, 2009) (Figure 17). The viewer allows the user to view the model in both plan and 3D perspective but it is the interrogation

tools that enable the creation of synthetic boreholes and cross sections at any location that are of importance here.
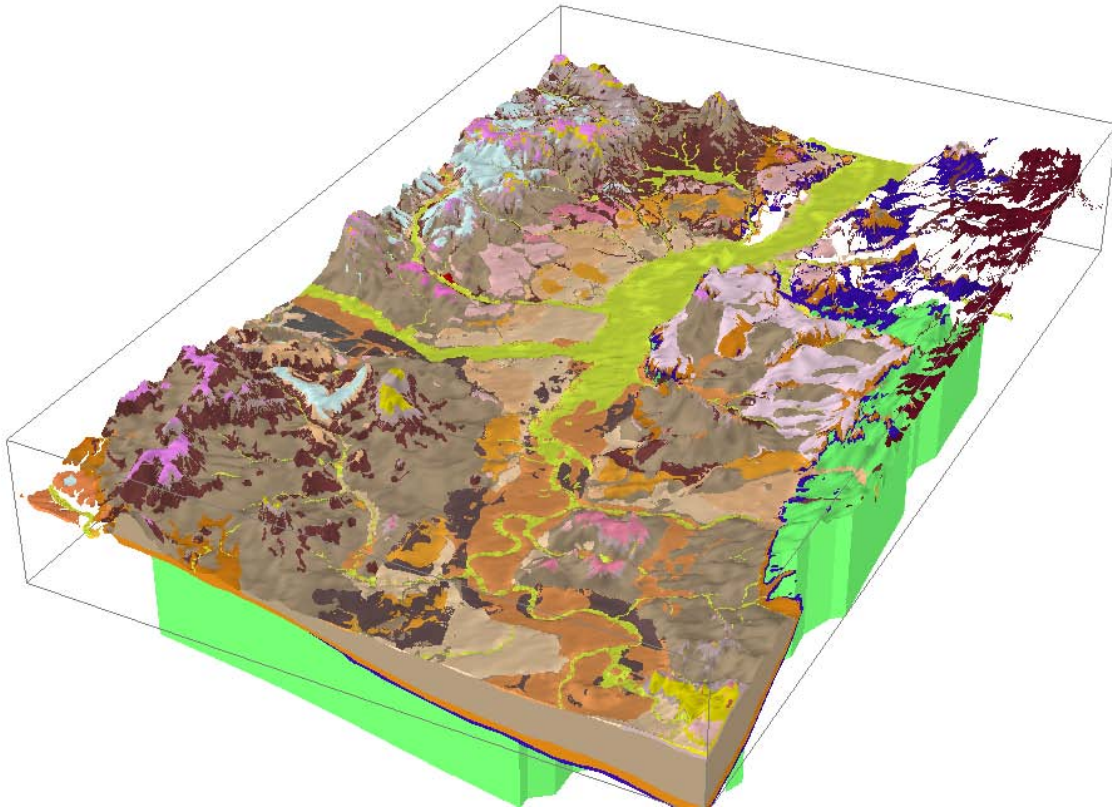
Figure 16. BGS London lithoframe50 geological model.
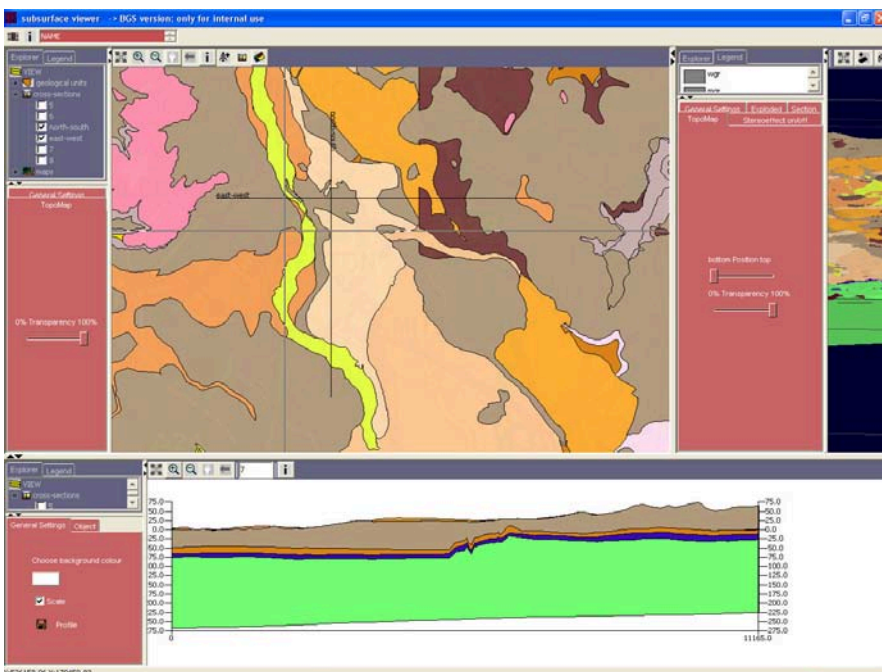
Figure 17. The subsurface viewer containing the London Lithoframe model.

For the location of each comparison point a synthetic borehole was created (Figure 18). From the synthetic boreholes the thickness of each geological unit was derived for each comparison location (Table 5). These values were input into the subsidence model.

Figure 18. Synthetic borehole
created for point (0,0).

Table 5. Unit thickness for comparison point 0,0.
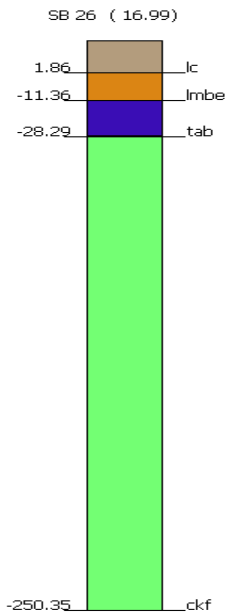
Geological Unit	Geology Code	Unit Thickness (m)
London Clay	lc	1.86
Lambeth Group	lmbe	9.5
Thanet Sands	tab	16.99
Chalk	ckf	222.06

4.3.2   Groundwater level change values

Values for groundwater levels came from the UK Environment Agency (EA). As mentioned in section 2, the EA produce a yearly report titled 'Groundwater Levels in the Chalk-Basal Sands Aquifer of the London Basin' which includes contour maps (for January each year) of groundwater level change. We were able to get access to the contour maps for January 1996 to January 2001, and January 2006. These maps were digitised and imported to the GIS. The following describes how groundwater data were obtained for each temporal resolution.

4.3.2.1 CASE 1

To obtain average groundwater values for the study period the groundwater level contours from 1997 and 2006 were differenced. The resultant grid dataset can be seen in the background data used in Figure 14. Values for the average change in groundwater levels for each comparison point were then read off from the grid square underlying comparison point in question.

4.3.2.2 CASE 2

Yearly changes in groundwater level values; for each of the six points used in this comparison, were derived from digital contour maps in the GIS. Table 6 shows an example of the yearly values for comparison point (0,0).

Year	GW yearly level change (m)	Total GW reduction (m)
1997	4	4
1998	5	9
1999	2.5	10.5
2000	3.5	14
2001	10	24

Table 6. Yearly groundwater values used for comparison point 0,0.

4.3.2.3 CASE 3

In the 2007 edition of the 'Groundwater Levels in the Chalk-Basal Sands Aquifer of the London Basin' Environment Agency report, a hydrograph (Figure 11) was published for the site of investigation. Accurate monthly groundwater levels were taken from this plot and used as input to the subsidence model.

4.4   PS DATA

The PS data used in this study was previously used in the London Land-levels study. Section 1 describes the data and the adjustments applied, of particular interest is that the data have been aligned with GPS and AG measurements to give absolute vertical ground velocity.

Since it cannot be guaranteed that PS points will be coincident with comparison points it was decided to consider all PS points within 100 m of the comparison point.

4.4.1   Case 1

For each comparison point, the velocity data for each PS point within 100 m was averaged over the 9 year period.

4.4.2   Case 2

For each of the six comparison points the PS data within 100 m were gathered. PS data were broken down into yearly data. The SLOPE function in Microsoft Excel was used to produce an average PS motion for each year.

It was assumed that at the start of the study period the terrain was at zero level, cumulative terrain motions were derived from the yearly rates, which could be directly compared with the model results. An example of the cumulative displacement derived by this method is shown in Figure 19.
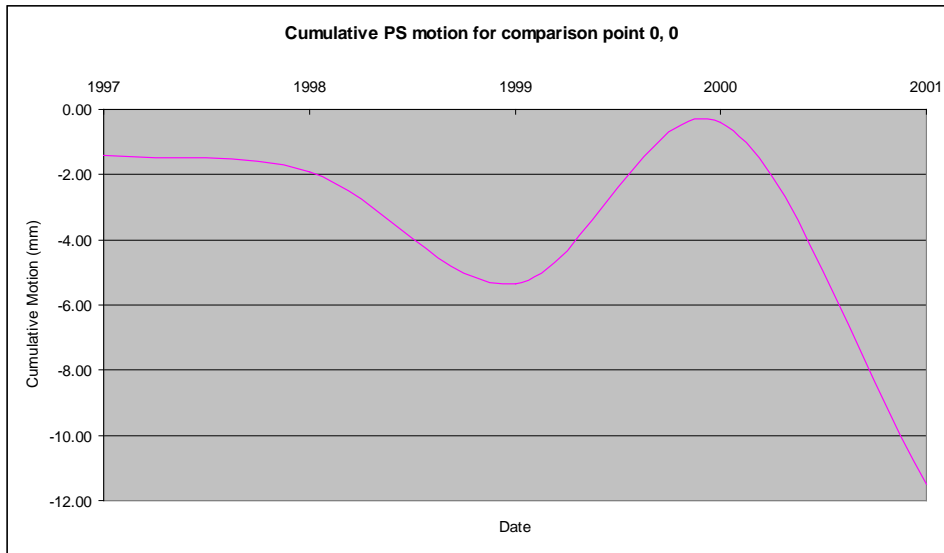
Figure 19. Cumulative PS motion derived for comparison point 0,0.

4.4.3   Case 3

For PS points within 100 m of Merton Abbey the mean motion for each date was calculated, effectively creating an average time series which can be compared to the model result.

5 Comparison Results

5.1   CASE 1 – STUDY PERIOD AVERAGES

Average PS rates and modelled subsidence rates, derived using average groundwater level changes, were compared for 22 points. The results are presented in Table 7 and Figure 20.

Point ID	Total PS subsidence 97-06 (mm)	Total modelled Subsidence 97-06 (mm)	Average rate of PS subsidence (mm/year)	Average rate of modelled Subsidence (mm/yr)	Difference in total	Difference in rate
0,0,	-18.3	-26.1	-2.0	-2.9	-7.7	-0.9
0,1	-18.9	-25.5	-2.1	-2.8	-6.6	-0.7
0,2	-3.4	-15.8	-0.4	-1.8	-12.5	-1.4
0,-1	-11.8	-14.7	-1.3	-1.6	-2.9	-0.3
0,-2	-14.0	-11.7	-1.6	-1.3	2.2	0.2
0,-3	-15.0	-11.1	-1.7	-1.2	3.9	0.4
0,-4	-17.0	-9.0	-1.9	-1.0	8.0	0.9
0,-5	-18.7	-10.1	-2.1	-1.1	8.6	1.0
0,-6	-18.4	-10.3	-2.0	-1.1	8.1	0.9
0,-7	-16.4	-4.5	-1.8	-0.5	12.0	1.3
1,-2	-9.4	-11.4	-1.0	-1.3	-1.9	-0.2
2,-2	-11.2	-10.3	-1.2	-1.1	0.9	0.1
3,-2	-8.1	-15.0	-0.9	-1.7	-6.9	-0.8
4,-2	-16.8	-9.6	-1.9	-1.1	7.3	0.8
5,-2	-19.5	-11.2	-2.2	-1.2	8.3	0.9
6,-2	-19.5	-9.2	-2.2	-1.0	10.2	1.1
7,-2	-10.1	-7.0	-1.1	-0.8	3.0	0.3
8,-2	-11.4	-13.5	-1.3	-1.5	-2.1	-0.2
.-1,-2	-15.9	-12.7	-1.8	-1.4	3.2	0.4
.-2,-2	-17.6	-12.3	-2.0	-1.4	5.3	0.6
.-3,-2	-20.6	-9.8	-2.3	-1.1	10.8	1.2
.-4,-2	-20.3	-10.3	-2.3	-1.1	10.0	1.1
			AVERAGE		6.48	0.72
			STANDARD DEVIATION		3.51	0.39
			VARIANCE		12.32	0.15

Table 7. The results of the comparison of average PS subsidence and average modelled subsidence for Jan 1997 to Jan 2006. Orange highlighting shows points near to Merton Abbey pumping station.

Rates of PS and modelled subsidence differ on by 0.72 mm/yr (average), over the 9 year study period, amounting to an average total difference in subsidence of 6.48 mm. The maximum

difference in rate is 1.4 mm/yr and the minimum 0.1 mm/yr. The data have a Root Mean Square Error (RMSE) of 0.547 mm/yr.
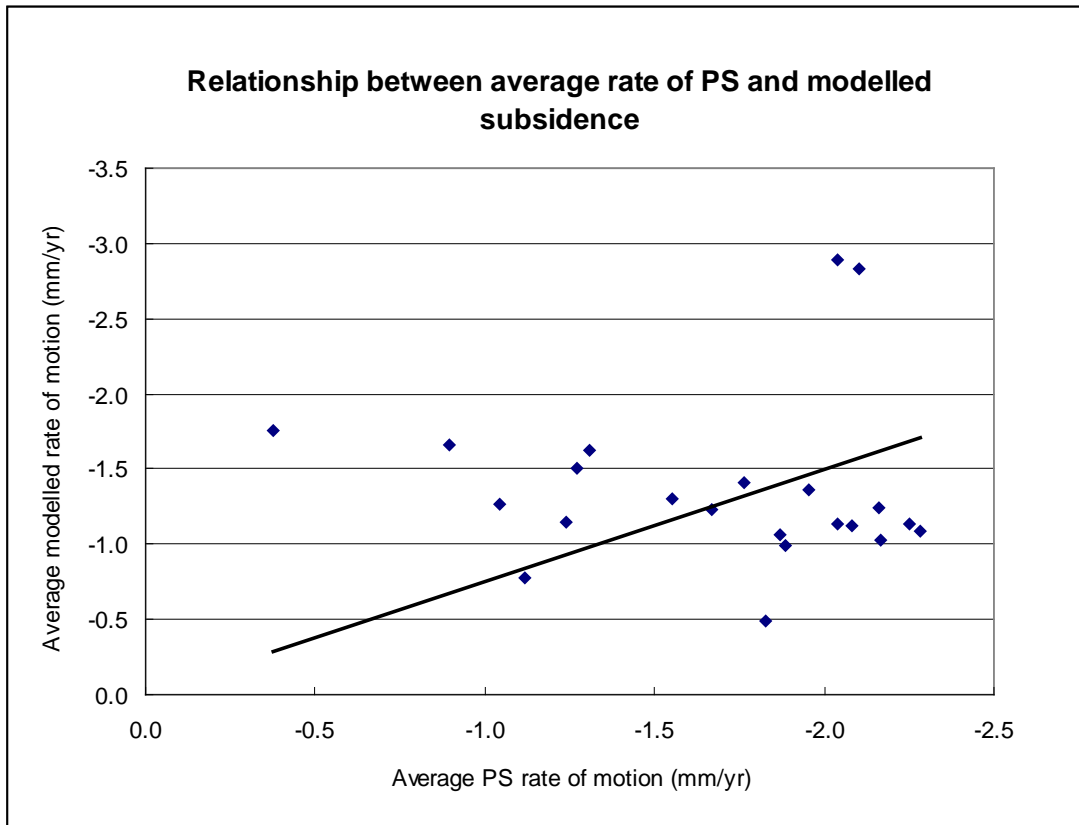
Figure 20. The relationship between the average rate of subsidence shown by the PS results and the modelled results.

The accuracy of the model relies on the accuracy of the groundwater level input. Groundwater levels in the London region are measured at specific boreholes only and the values interpolated to form the contour maps used. It is therefore to be expected that the accuracy of the measurements will decrease with distance from the borehole. Figure 21 shows that a positive relationship exists between the PS and model difference results and the distance from the Merton Abbey pumping station where measurements were made.
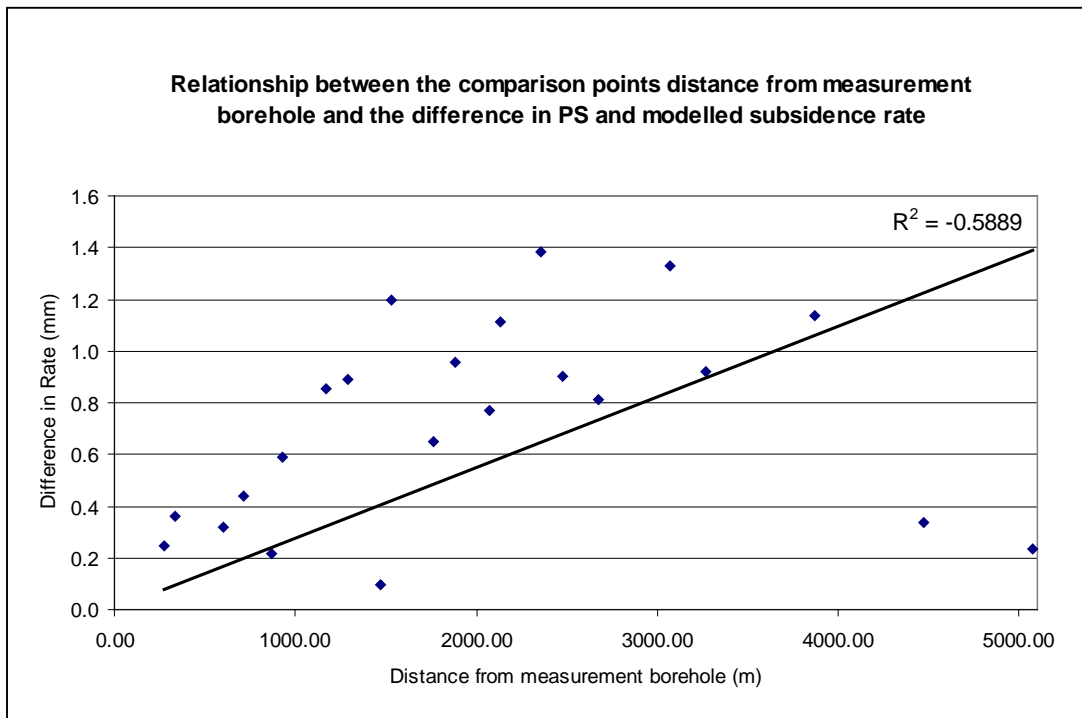
Figure 21. Relationship between the difference in subsidence rates and the distance of the comparison points from the measurement borehole at Merton Abbey.

If only points closest to the Merton Abbey borehole, where the groundwater values are likely to be most accurate, are considered the comparison results improve to an average difference in rate of 0.33 mm/yr and a total difference of 3 mm (orange rows in Table 7). The maximum difference in rate is 0.4 mm/yr and the minimum 0.2 mm/yr. The data have an RMSE of 0.143 mm/yr.

5.2   CASE 2

Cumulative subsidence figures derived from the PS time series were plotted against the cumulative motions derived from the model when run with yearly groundwater values.
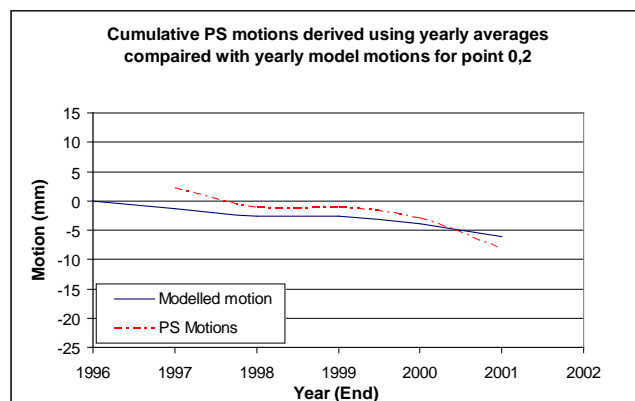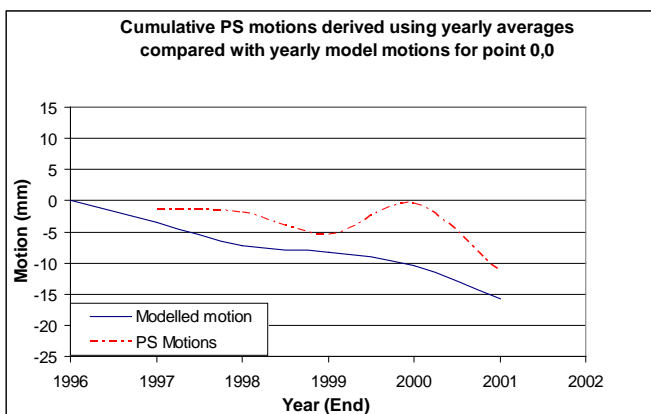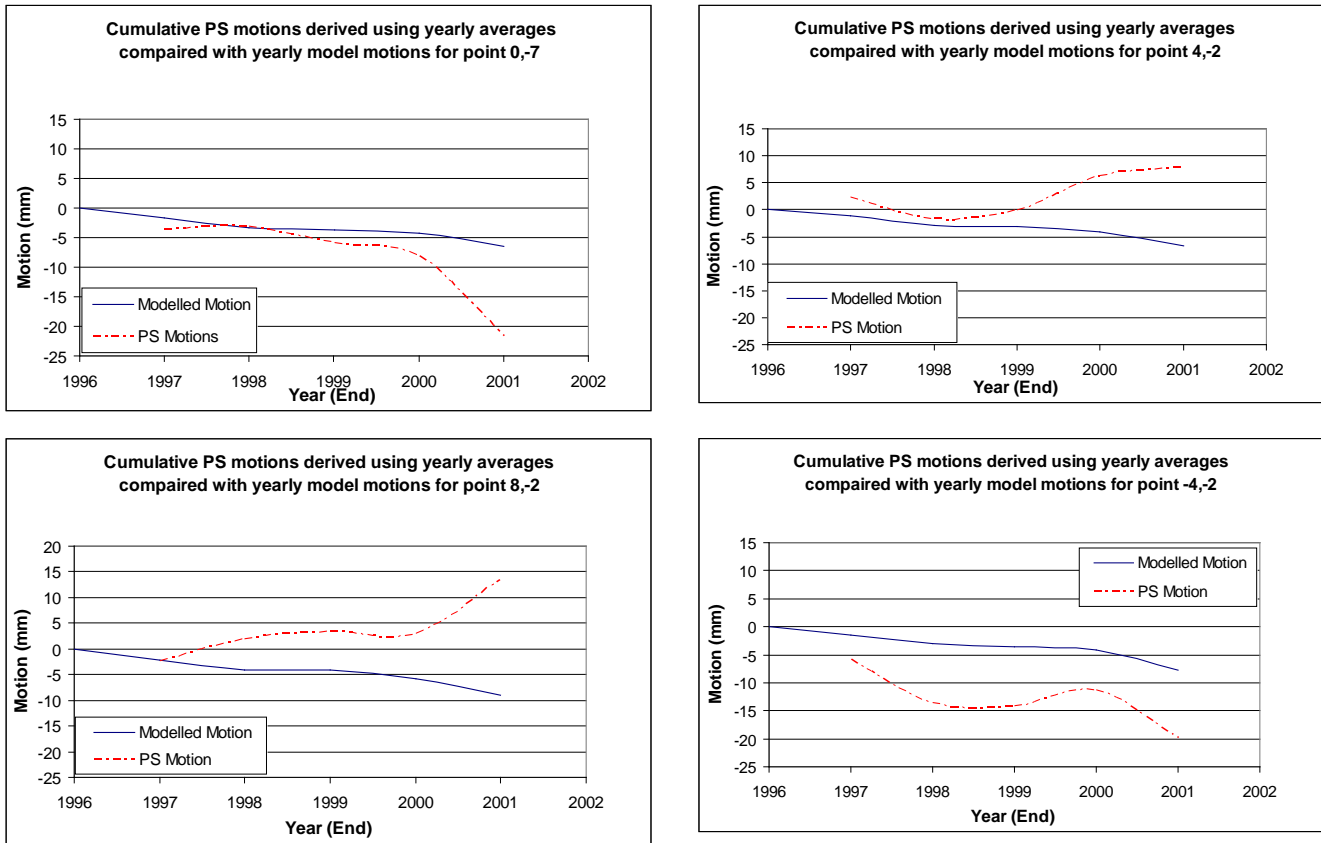
Figure 22. Comparison plots for the six comparison points at which the subsidence model was run using yearly groundwater levels as an input.

The best agreement is shown by point (0,2) in Figure 22, it is interesting to note that this is the point that shows the least agreement when average PS and model results were compared in case 1.

The modelled motions for each point follow a similar profile. No uplift is predicted by the model for these points in this time frame since groundwater levels were decreasing each year. Where PS data indicates uplift this may be attributed to some process other than groundwater abstraction. In many cases the plots show similar trends for the PS and model results. The overall shape of the model and PS plots for (0,0), (-4,-2) and (0,-7) are similar. For these points; where the PS data are indicating an uplift the model is predicting a flattening off of the subsidence rate. This implies that there is may be a competing uplifting factor in the region, the effect of which is suppressed during times of increased groundwater abstraction.

Point (8,-2) (Figure 22) shows the least agreement; this is the furthest point from the groundwater measurement location. This point also exhibits the PS uplift at times of a lessening of the modelled subsidence.

Points (0,-7), (4,-2) and (8,-2) show the widest departure between model results and PS results in 2001. In 2001 only three radar images were available to process and these were poorly distributed throughout the year; in January, July and August. The least squares fit used to produce a yearly average is therefore based on a limited number of poorly spaced samples. It is likely that short time span motions are missed and averaged out.

Cumulative subsidence figures for each year were derived from the PS time series by totalling the yearly motion rates. These were compared with the cumulative modelled motions. The average difference between these two total motions is given in Table 8, along with the root mean square error values.

31

Point	Average difference between PS and model 1997-2001 (mm)	RSME 1997 - 2001	Average difference between PS and model 1997-2000 (mm)	RSME 1997 - 2000
0,0	4.09	2.61	4.05	1.87
0,2	1.55	0.31	1.44	0.35
0,-7	3.93	2.85	1.66	1.33
4,-2	5.40	2.59	3.56	2.83
8,-2	7.43	1.45	4.47	1.22
.-4,-2	7.45	2.02	6.53	2.17
	Average RMSE	1.97		1.63

Table 8. Average differences between the PS results and model results when using yearly groundwater levels.

Although the plots in Figure 22 present a poor comparison the maximum average difference, for each point, between the yearly modelled result and PS average is just 7.45mm and the minimum is 1.55 mm, the average RMSE is just 1.97mm a year. If 2001 data are omitted from this analysis then the results improve, this is probably due to the small number of radar images available for 2001 and the poor temporal sampling this presents to the PS analysis.

Year	Average difference for all points (mm)
2001	11.76
2000	6.81
1999	4.60
1998	4.10
1997	2.59

Table 9. Average, for all six points, yearly difference between the modelled subsidence and the PS derived yearly subsidence.

The maximum difference between the cumulative model and PS results is 22.2 mm, this occurs for point (8,-2) in 2001. The minimum difference is 0.17 mm, which is also at point (8,-2) but for 1997, as Table 9 shows the average difference, for all points, between the modelled and PS derived yearly subsidence increases with time and is at its greatest in 2001. This is likely to be related to problems with the method of deriving average yearly motions from the PS data, which is a measure better computed within the PS processing chain.
.

5.3   CASE 3

The Hydrograph for Merton Abbey (Figure 9) has made it possible to directly compare the PS time series with a model result where the groundwater input is monthly.
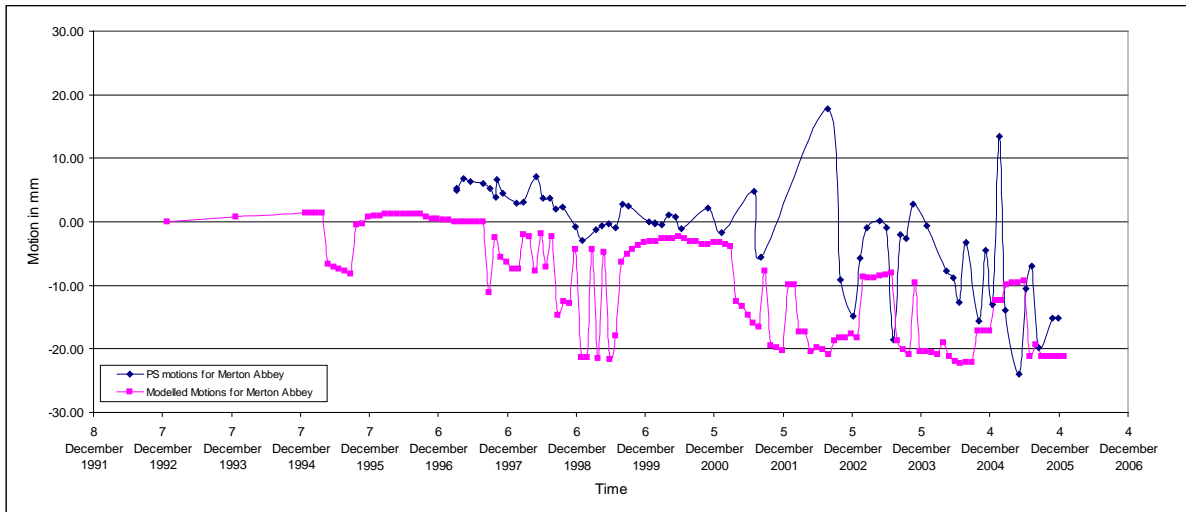
Figure 23. Comparison of monthly modelled subsidence (magenta) and PS time series (blue) at Merton Abbey pumping station

Figure 23 shows a visual comparison between the monthly modelled motions and the PS time series for the Merton Abbey pumping station. There is a general offset, which can be corrected for by setting the reference date for the time series to the same as the first date in the time series in 1997.
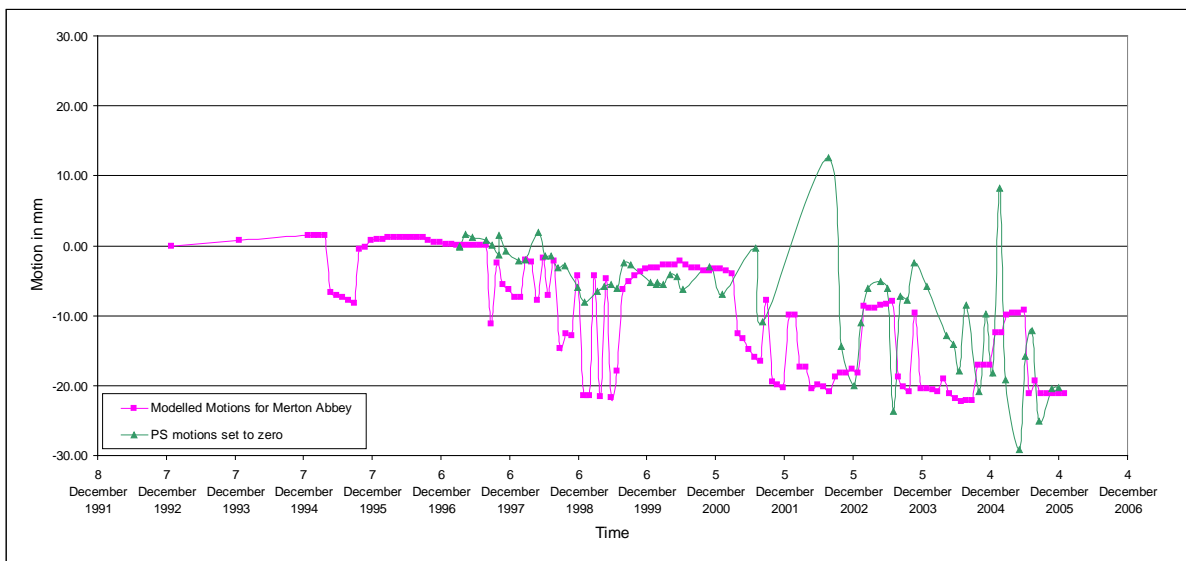
Figure 24. Comparison of monthly modelled subsidence (magenta) and PS time series which have been set to zero (green) at Merton Abbey pumping station

With the PS data set to zero in 1997 (Figure 24), the comparison is easier and the similarities are more noticeable. Many periods of uplift and subsidence are coincident and in many cases they are of similar magnitudes and even values. For example at the start of 2003 both datasets show uplift, followed by a plateau of motions and then subsidence.

In general the comparison is better for the first 5 years. The episodic pumping that takes place at this pumping station during 1998 and 1999 (Environment Agency, 2007) is evident in the modelled motions. PS motions do indicate that the terrain is fluctuating during 1998 and 1999 however the

magnitudes of these fluctuations are not of the same scale as those seen in the model results. This muted response of the PS is possibly a response to other factors influencing the terrain motion. The fact that the episodic pumping is picked up by the PS at all is encouraging for both the accuracy of the model and that of the PS data.

The PS time series once again shows anomalous measurements in 2001 and 2002. The 2002 peak is the greater but it is coincident with a peak of uplift in the model results, while the peak of uplift shown by the PS in 2001 is coincident with a period of subsidence in the model results. As discussed earlier, only three radar scenes were processed for 2001 the same is true for 2002, this may suggest that PS results are more reliable when the temporal sampling is greater. However there are also large fluctuations in PS motions in 2004, here the PS motions indicate rapid uplift followed by rapid subsidence while the modelled motions show a constant period of uplift. It may be that during this period groundwater was not being abstracted, and so was not controlling terrain motions, another factor is overprinting the groundwater induced motion with that of subsidence.

Direct comparison of the motion figures is not possible since the dates when groundwater levels were measured and radar scenes were acquired are not coincident. Statistically the two datasets are very similar; the average rate of motion for the PS is -1.87mm/yr and for the modelled motions it is -1.86mm/yr, which is a remarkable difference of just 0.01mm/yr.

5.4   THE USE OF PS DATA TO IMPROVE THE MODEL

Figure 25 emphasizes the similarity between the modelled and PS motion rates through the best-fit trend lines. It also becomes apparent that shifting one of the datasets in time would result in a near perfect match.
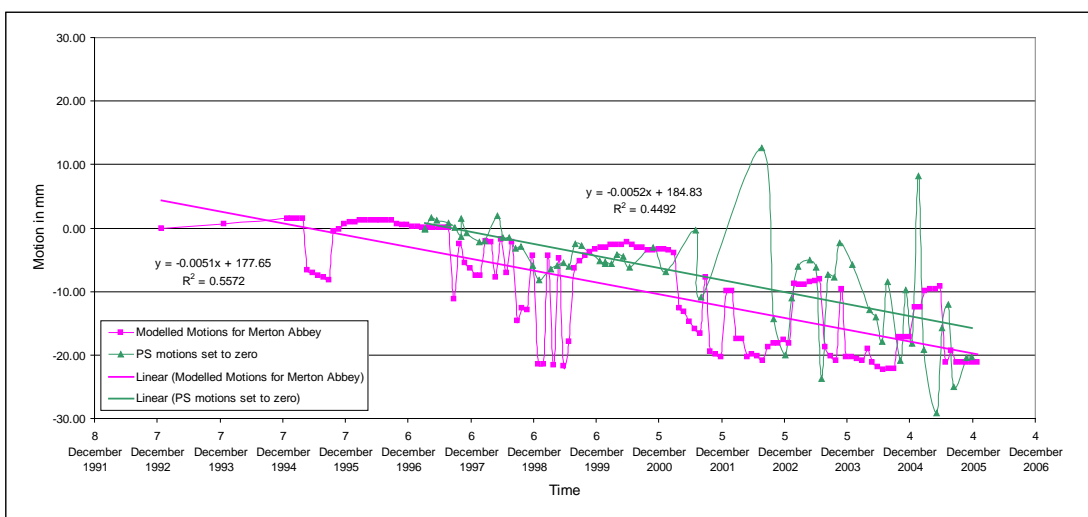
Figure 25. Modelled motions and PS motions for Merton Abbey with trend lines displayed.

When the model was written no account was taken of time-lag; that is the amount of time that it would take for each geological unit to compact in response to the removal of water. Instead it was assumed that this effect would be instantaneous. To calculate time-lag, the vertical conductance of the beds must be known. The calculated time-lag for the Chalks and Thanet Sands is less than one

month. However in the literature (Shi et al., 2007; Shearer, 1998; Poland, 1984; Bell et al., 1986; Li et al, 2006) the vertical conductance for the materials similar to that in the Lambeth Group is wide ranging (2.33×10^{-3} m/day and 6.7×10^{-7} m/day) giving a time lag for consolidation of the Lambeth Group ranging from 3 days to 33 years. We could not get an accurate value without completing laboratory tests on samples from the study site.

Assuming that the compaction time lag is the only factor responsible for the observed difference in modelled and PS motions then comparison plots such as Figure 25 allow the time lag to be calculated. If a time lag of two years is assumed then the best-fit lines for each series become coincident (Figure 26).
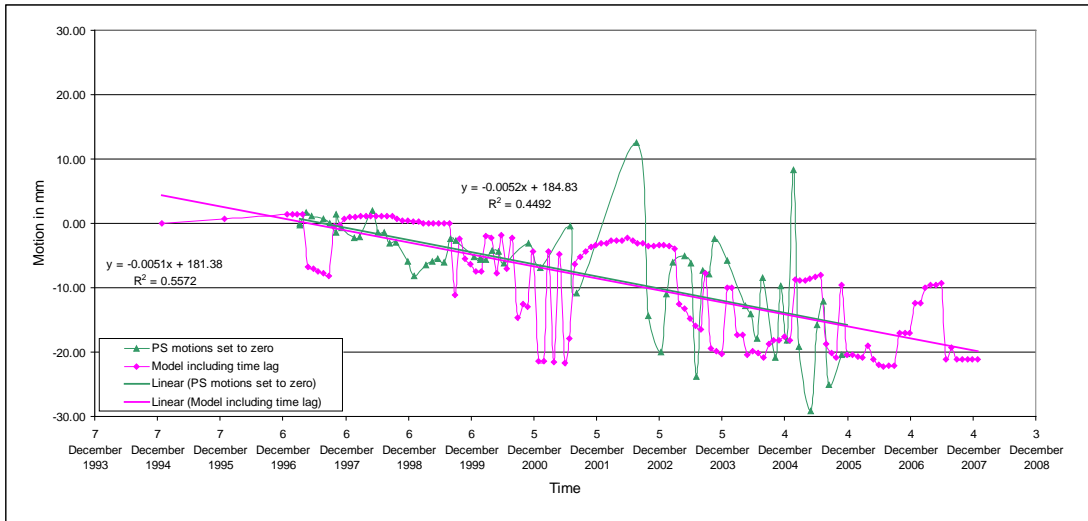
Figure 26. Modelled motion with a time lag of two years plotted against PS motions. Best-fit lines for each dataset now overlie.

6 Sources of Error

6.1   LIMITATIONS OF THE MODEL

As previously mentioned, the time-lag for compaction of the geological units following water abstraction has not been included in the model. The time-lag will vary for each unit and published figures (Shi et al., 2007; Shearer, 1998; Poland, 1984; Bell et al., 1986; Li et al, 2006) vary considerably, the only way to ensure that accurate time-lags are used is to conduct laboratory measurements of sample from the study site. It has been shown that the time-lag can be deduced from the PS data therefore overcoming the time lag issue via use of the PS data.

The compressibility index of each geological unit used was based on figures derived by comparison to several subsidence measurement studies (Shi *et al.*, 2007; Kitching and Shearer, 1995; Bell *et al.*, 1986; and Poland, 1984). Since the index values are not accurately determined for each unit via laboratory measurements there will be an error associated with them. Due to the heterogeneous and anisotropic nature of the formations (clay, silt, and sand), compression indices will vary widely depending on location and depth. It would therefore be necessary to carry out extensive laboratory tests to determine the properties at different depths for each modelled location.

The model assumes a homogeneous matrix, average density and initial porosity based upon sediment type and depth of burial. These assumptions, while approximating the unit as a whole, do not account for local variations, which may influence the modelled behaviour. The BGS have a geotechnical database which has information on many formations. The data has been built up through testing of material derived mainly via shallow site investigation boreholes. Initially these data were not used as model input as they were not thought to be representative of the unit characteristics at depth. Porosity values from the database were used as input and the model re-run for certain locations. The model results shown negligible differences in predicted subsidence and the resulting conclusions were the same. Any future work using this model would make more use of this data.

The confining London Clay that overlays the other formations may affect the translation of underlying unit consolidation into surface subsidence. It is expected that the Clay will have an *averaging* effect on the surface subsidence due to its plastic nature. The averaging will vary at different locations, depending on the thickness of the Clay and the compaction rates of the other formations. To approximate this averaging effect the total compaction data was smoothed using a 7-point moving average (trend). The results are given in Figure 27, however it should be noted that an *ad hoc* approach has been applied to the level of smoothing, and therefore these results should be interpreted as such.
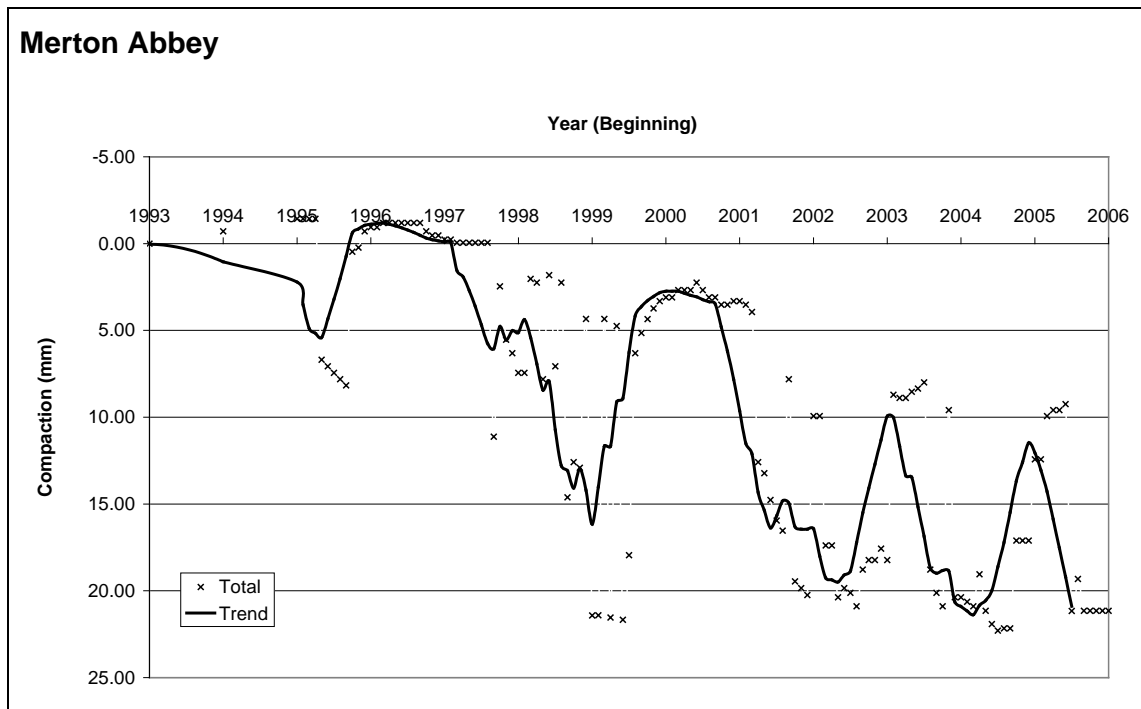
Figure 27. Possible surface movement: The smoothing effects that the confining clay layer may impose on the translation of underlying compaction into surface subsidence have been added to the modelled results.

A further source of error in the modelled motions arises from the groundwater data used as input. These levels have been derived via measurements in several boreholes across London (Environment Agency, 2007). Interpolation methods have been used to fill in between boreholes. The interpolation can never be a substitute for real measurements and does not take account of the controlling factors such as Faulting.

The subsidence model does not make any provision for the control of faults on groundwater flow. The study area is bounded to the northwest by the Wimbledon Fault and as such the fault should have limited effect on the subsidence within the study area. If the model was to be applied to the northwest of the fault line then it would require modification. Groundwater levels used in this work are derived with no account for the faults influence.

6.2   LIMITATIONS OF THE PS DATA

Potential errors in the PS data have been reduced during the London Land-levels project where several of the common sources of error in PS datasets were addressed. The reference point was moved to a stable location, line-of-sight measurements were projected to the vertical and PS data were tied to AG and GPS measurements to give absolute, rather than relative, velocities. These corrections do assume that motions had no horizontal components and that the area of chalk bedrock selected as a stable point was stable.

In the yearly and monthly comparisons it was noted that 2001 and 2002 showed marked differences. It is reasoned that this is due to the limited number of radar images available for these dates and hence the limited temporal sampling of the PS data for these years.

PS measurements are measurements of the surface as seen by the radar. This can be the ground surface or any part of the features on the ground surface. A PS measurement can therefore be of the top of a building. This leads to problems when making comparisons with the model outputs, which predict motions of the ground surface. For the above example a difference between the PS and modelled motions could be due to a motion within the buildings structure, which will be present in the PS data but not predicted by the model.

When considering the results it is most important to remember that PS measurements are of the total motion for any given point, where as the modelled motions are only for ground motion thought to occur due to measured groundwater level changes. The fact that the agreement is so good implies that groundwater level changes are by far the strongest factor leading to ground motions in this area.

7 Conclusions

7.1   CASE 1 - AVERAGE COMPARISON

Average rates of PS and modelled subsidence for 1997 to 2006 differ on average by 0.72 mm/yr, amounting to an average total difference in subsidence of 6.48 mm. The data have an RMSE of 0.55 mm/yr.

For the points closest to the Merton Abbey borehole, where the groundwater values used in the model are likely to be most accurate, the average difference in rate is 0.33 mm/yr and the difference of total subsidence is 3 mm. The data have an RMSE of 0.14 mm/yr

7.2   CASE 2 - YEARLY COMPARISON

The yearly comparison is not as favourable as the 9 year average comparison; this is probably due to:

- An under sampling in time for the PS data, where short term motions are not represented. Over the yearly period considered here these short term motions provide a higher contribution.

- Other motion inducing factors which may overprint the groundwater induced motion. This seems to be the case for several of the comparison points where the PS data show uplift while the model is predicting a levelling off of subsidence.

The monthly and study-period average comparisons were favourable; this has highlighted the difficulty in deriving yearly averages from the PS data. This parameter would probably be better derived at time of PS processing.

7.3   CASE 3 - MONTHLY COMPARISON

The visual comparison of PS time series and modelled motions for Merton Abbey shows that although there are some discrepancies the overall fit is good. Many of the motion features are present in both datasets. When the time series is shifted the linear best-fit of each data is almost identical.

For the comparison at Merton Abbey pumping station there is a difference in average rates of motion of 0.01 mm/yr.

7.4   OVERALL CONCLUSIONS

A simple model has been constructed, which calculates the amount of strata compaction due to a change in piezometric level (and resulting hydrostatic pressure change). The model has been successfully applied at several locations within the Thames Basin, centred on Croydon, London, UK. The model has been run with differing complexities of input piezometric level, and for varying periods of time. It takes into account the properties of the underlying geology, by separating the subsurface into formations that are considered homogenous. For the Terrafirma project, the formation properties were inferred using the London Basin model and various literatures. The model output is shown to be highly dependant on the piezometric level; however factors such as the overburden properties also affect the compaction rates for a unit.

The comparison of modelled and PS motion has proved successful giving confidence in both the model and the PS data. Each approach to terrain motion measurement has it's limitations but this

work has shown that they can produce similar results and that a combination of methods is often better than one alone. A contributing factor to the success seen here has been the projection of the PS data to the vertical and the transformation to absolute motions through incorporation of the GPS data (Bingley et al, 2007). This is turn has meant that the PS data could then be used to improve the model via comparison of linear averages and the computation of a shift required for the modelled data to fit the PS. This shift represents the time-lag effect of compaction of geological units following groundwater abstraction, an input required by the model, but one that would be expensive to determine by other means.

It must be remembered that the model presented here was written specifically for the geology of the area and can only predict ground motions relating to groundwater level fluctuations. It would be fairly easy to transport the model to areas of different geology. Building in other motion inducing factors is possible but would be a complicated process.

8 Abbreviations

a_v	coefficient of compressibility
b	interbed thickness
c_c	compressibility index
e	new void ratio
e_0	initial void ratio
H	unit thickness
k_z	vertical conductivity
m_v	coefficient of volume compressibility
n_0	initial porosity
p	geostatic pressure
p_s	new effective stress
p_{s0}	initial effective stress
p_w	pore fluid pressure
Ss	specific storage
τ	aquitard time constant
GPS	Global positioning System
AG	Absolute Gravity
PSI	Persitant Scatterer interferometry
RMSE	Root Mean Square Error

9 References

BINGLEY, R M, TEFERLE, F N, ORLIAC, E J, DODSON, A H, WILLIAMS, S D P, BLACKMAN, D L, BAKER, T F, RIEDMANN, M, HAYNES, M, ALDISS, D T, BURKE, H C, CHACKSFIELD, B C, and TRAGHEIM, D G. 2007. Absolute fixing of tide gauge benchmarks and land levels: Measuring changes in land and sea levels around the coast of Great Britain and along the Thames Estuary and River Thames using GPS, absolute gravimetry, Persistent Scatterer Interferometry and tide gauges. *Department of Environment, Food and Rural Affairs R&D Technical Report*, FD2319/TR. Available from:
http://www.defra.gov.uk/science/project_data/DocumentLibrary/FD2319/FD2319_5408_TRP.pdf

BINGLEY, R M, TEFERLE, F N, ORLIAC, E J, DODSON, A H, WILLIAMS, S D P, BLACKMAN, D L, BAKER, T F, RIEDMANN, M, HAYNES, M, PRESS, N, ALDISS, D T, BURKE, H C, CHACKSFIELD, B C, TRAGHEIM, D, TARRANT, O, TANNER, S, REEDER, T, LAVERY, S, MEADOWCROFT, I, SURENDRAN, S, GOUDIE, J R, and RICHARDSON, D. 2008. The measurement of current changes in land levels as input to long term planning for flood risk management along the Thames estuary and River Thames. *Coastal Engineering*.

BELL, F. G., CRIPPS, J. C., and CULSHAW, M. G., 1986: A review of the engineering behaviour of soils and rocks with respect to groundwater. *Groundwater and Engineering Geology*, 3, 1-23.

DOBRYNIN, V. M., 1962: Effect of overburden pressure on some properties of sandstones. BGS, UK.

ELLISON, R A, WOODS, M A, ALLEN, D J, FORSTER, A, PHAROAH, T C, And KING, C. 2004. Geology of London. Memoir of the British Geological Survey, Sheets 256 (North London), 257 (Romford), 270 (South London) and 271 (Dartford) (England and Wales).

ENVIRONMENT AGENCY, 2007. Groundwater Levels in the Chalk-Basal Sands Aquifer of the London Basin, Unpublished report.

JACOB, C. E., 1940: On the flow of water in an elastic artesian aquifer. *Transactions of the American Geophysical. Union*, 2, 574-586.

KITCHING, R., and SHEARER, T. R., 1995: Modelling of Subsidence Due To Groundwater Extraction. British Geological Survey Technical Report, WC/95/42.

GUPTA, S. C., and LARSON, W. E., 1979: Estimating soil water retention characteristics from particle size distribution, organic matter percent, and bulk density. *Water Resources Research*, 15, 1633-1635.

LI, C., TANG, X., and MA, T., 2006: Land subsidence caused by groundwater exploitation in the Hangzhou-Jiaxing-Huzhou Plain, China. *Journal of Hydrogeology*, 14, 1652-1665.

MEINZER, O. E., 1928: Compressibility and elasticity of artesian aquifers. *Economic. Geology*, 23 (3), 263-291.

POLAND, J. F., 1984: Guidebook to studies of land subsidence due to ground-water withdrawal. Unesco, Paris, France.

RILEY, F. S., 1969: Analysis of borehole extensometer data from central California. *in* Tison, L.J. *Land Subsidence*. International Association of Scientific Hydrology Publication., 89, Vol 2, 423-431.

SHEARER, T. R., 1998: A numerical model to calculate land subsidence, applied at Hangu in China. *Engineering Geology*, 49, 85-93.

SHI, X. -Q., XUE, Y. -Q., YE, S. -J., WU, J. -C., ZHANG, Y., and YU, J., 2007: Characterization of land subsidence induced by groundwater withdrawals in Su-Xi-Chang area, China. *Environmental. Geology.*, 52, 27-40.

TERRINGTON, R.L.; MATHERS, S.J.; KESSLER, H.; HULLAND, V.; PRICE, S.J.. 2009 *Subsurface viewer 2009 : user manual V1.0.* Nottingham, UK, British Geological Survey, 23pp. (OR/09/027) (Unpublished)

TERZAGHI, K., 1925: Principles of soil mechanics: IV, Settlement and consolidation of clay. *Engineering News Record.*, 874-878.

ZIMMERMAN, R. W., 1991: Compressibility of Sandstones. Elsevier Amsterdam, NL. 173pp.